AD-A031 733 DAVID W TAYLOR NAVAL SHIP RESEARCH AND DEVELOPMENT CE--ETC F/G 20/4
SIMILARITY-LAW ENTRAINMENT METHOD FOR TWO-DIMENSIONAL TURBULENT--ETC(U)
DEC 75 P S GRANVILLE

UNCLASSIFIED DTNSRDC-4657 NL

1 OF 1
AD A031733

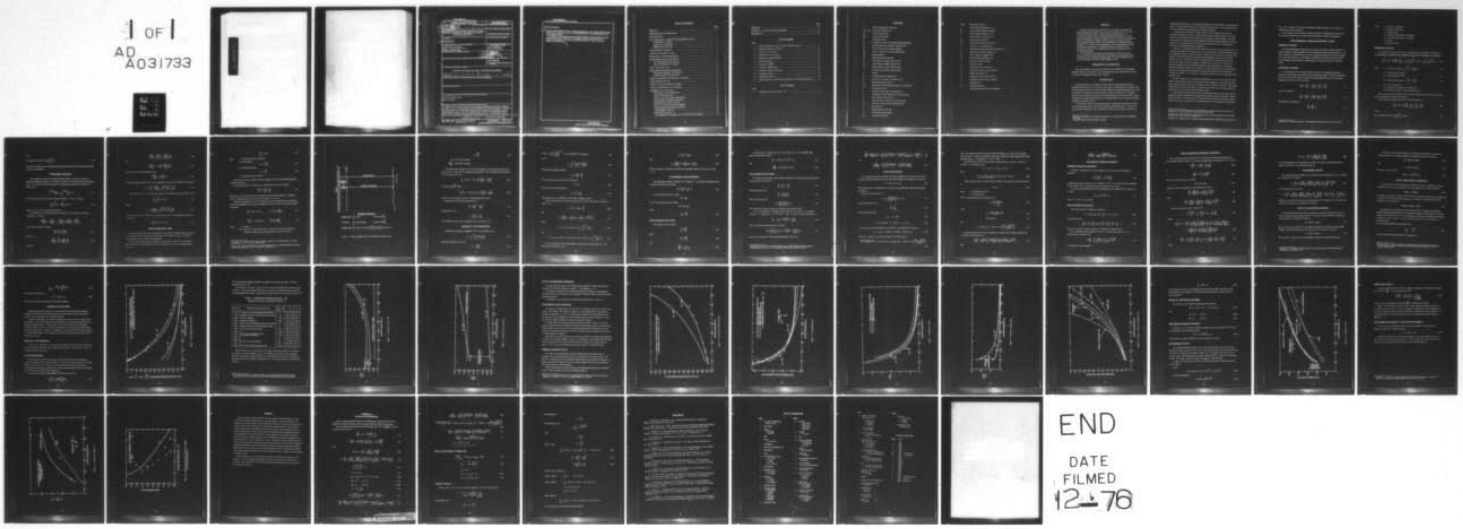

END

DATE FILMED
12-76

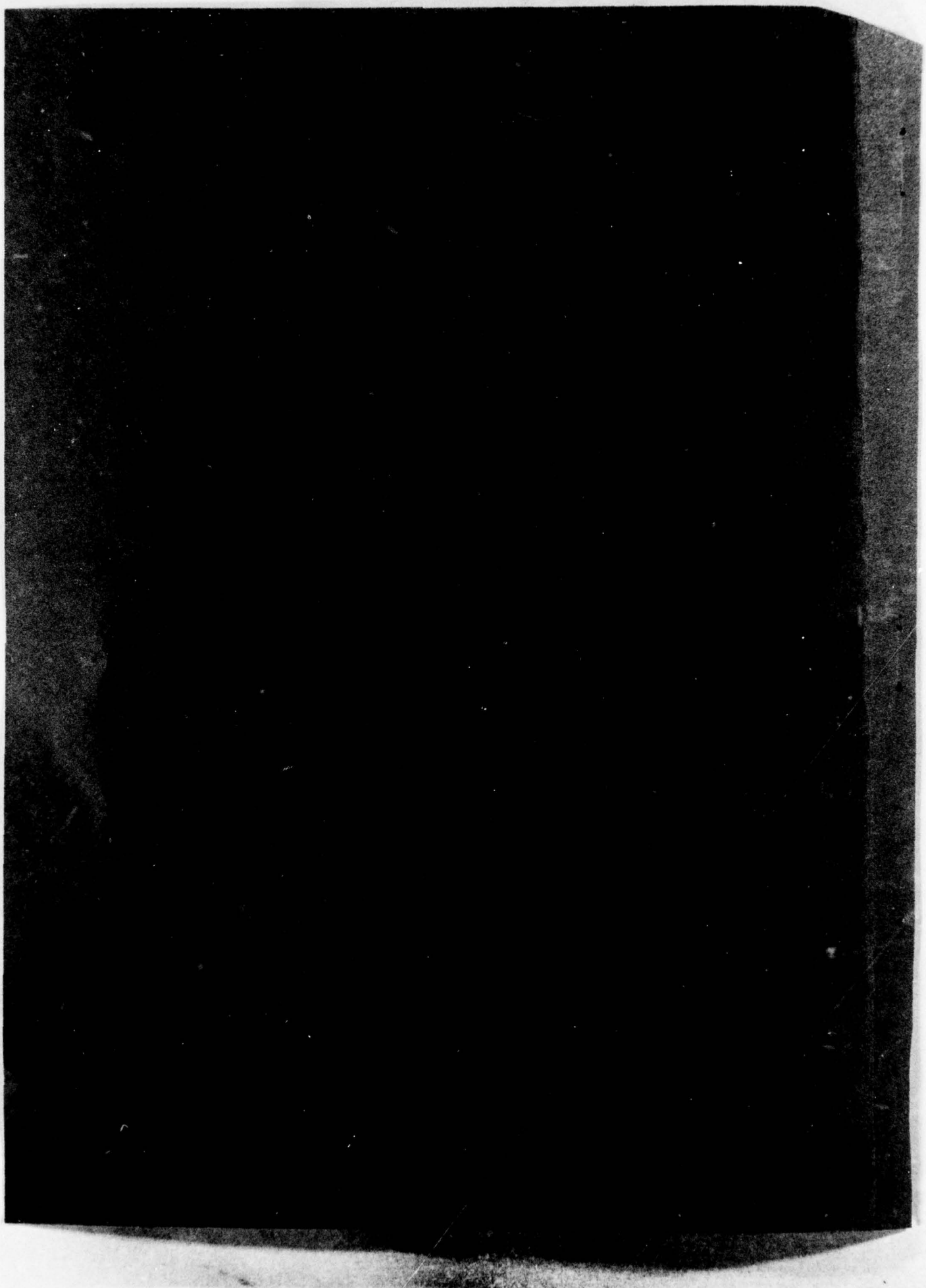

UNCLASSIFIED

SECURITY CLASSIFICATION OF THIS PAGE (When Data Entered)

REPORT DOCUMENTATION PAGE	READ INSTRUCTIONS BEFORE COMPLETING FORM
1. REPORT NUMBER: DTNSRDC [redacted]4657 (14)	2. GOVT ACCESSION NO. / 3. RECIPIENT'S CATALOG NUMBER
4. TITLE (and Subtitle): (6) SIMILARITY LAW ENTRAINMENT METHOD FOR TWO-DIMENSIONAL TURBULENT BOUNDARY LAYERS IN PRESSURE GRADIENTS,	5. TYPE OF REPORT & PERIOD COVERED / 6. PERFORMING ORG. REPORT NUMBER
7. AUTHOR(s): (10) Paul S. Granville	8. CONTRACT OR GRANT NUMBER(s)
9. PERFORMING ORGANIZATION NAME AND ADDRESS: David W. Taylor Naval Ship / Research and Development Center / Bethesda, Maryland 20084	10. PROGRAM ELEMENT, PROJECT, TASK AREA & WORK UNIT NUMBERS: Project ZR-023-0101 / Work Unit 1-1541-002
11. CONTROLLING OFFICE NAME AND ADDRESS (11)	12. REPORT DATE: Dec[redacted]75 / 13. NUMBER OF PAGES (12) 47 pp. 48
14. MONITORING AGENCY NAME & ADDRESS (if different from Controlling Office)	15. SECURITY CLASS. (of this report): UNCLASSIFIED / 15a. DECLASSIFICATION/DOWNGRADING SCHEDULE

16. DISTRIBUTION STATEMENT (of this Report)

APPROVED FOR PUBLIC RELEASE: DISTRIBUTION UNLIMITED

(9) Research and development rept.,

17. DISTRIBUTION STATEMENT (of the abstract entered in Block 20, if different from Report)

18. SUPPLEMENTARY NOTES

19. KEY WORDS (Continue on reverse side if necessary and identify by block number)

Turbulent Boundary Layer

Pressure Gradient

20. ABSTRACT (Continue on reverse side if necessary and identify by block number)

Analytical relations have been derived for calculating a developing two-dimensional turbulent boundary layer in a pressure gradient from two simultaneous differential equations: momentum and shape parameter. An entrainment method is used to obtain the shape parameter equation. Both equations incorporate the velocity similarity laws that provide a two-parameter velocity profile general enough to include any range of Reynolds numbers. The entrainment factor is based on the characteristics of equilibrium pressure gradients in a way which can accommodate → next page

387682

(Continued on reverse side)

DD FORM 1 JAN 73 1473 EDITION OF 1 NOV 65 IS OBSOLETE S/N 0102-014-6601

UNCLASSIFIED

SECURITY CLASSIFICATION OF THIS PAGE (When Data Entered)

(Block 20 continued)

the usual pressure gradients found in engineering applications. The method includes a newly formed wake modification function for the similarity laws as well as added effects due to low Reynolds numbers.

The variation of momentum loss boundary-layer thickness, local skin friction, and local velocity profile may be calculated for the boundary layers on hydrofoils and two-dimensional appendages. The various formulations are shown to correlate well with available experimental data.

TABLE OF CONTENTS

LIST OF FIGURES

LIST OF TABLES

NOTATION

A	Slope of logarithmic velocity law
a_1, a_2, a_3	Constants in Equation (77)
B_1	Law-of-the-wall factor
B_2	Velocity-defect factor
E	Entrainment factor
E_e	Entrainment factor for equilibrium pressure gradients
G	Rotta-Clauser shape parameter, Equation (38)
$\tilde{G}$	Part of G affected by pressure gradients
ΔG	Part of G affected by low Reynolds number
H	Shape parameter
$\tilde{H}$	Entrainment shape parameter
I_1	Velocity-defect integral, Equation (33)
I_2	Velocity-defect integral, Equation (36)
M	Pressure-gradient factor, Equation (88)
n	Exponent in power-law velocity profile
p	Pressure
$\hat{p}$	Cross-pressure term, Equation (9)
p_δ	Pressure at outer edge of boundary layer
q	Wake-modification function
R_θ	Momentum thickness Reynolds number, Equation (47)
s	Streamwise distance
U	Velocity at outer edge of boundary layer
u	Streamwise velocity component in boundary layer
u_τ	Shear velocity, Equation (24)
v	Normal velocity component in boundary layer
v_δ	Value of v at outer edge of boundary layer
w	Wake function
y	Normal distance from wall
y^*	Inner-law Reynolds number
y_o^*	Inner limit of log law

$(y/\delta)_1$	Outer limit of log law
α	Factor defined in Equation (71)
β	Clauser pressure-gradient parameter
$\bar{\beta}$	Factor defined in Equation (72)
γ	Factor defined in Equation (73)
δ	Boundary-layer thickness
δ^*	Displacement thickness, Equation (7)
ϵ	Correction in σ, Equation (69)
η	Similarity-law Reynolds number, Equation (29)
θ	Momentum thickness, Equation (5)
λ_1	Factor defined in Equation (42)
λ_2	Factor defined in Equation (43)
ν	Kinematic viscosity of fluid
ρ	Density of fluid
σ	Local skin-friction coefficient
$\tilde{\sigma}$	Turbulent normal stress in y-direction
$\bar{\sigma}$	Approximate value of σ
$\hat{\sigma}$	Normal stress term, Equation (10)
σ_t	Turbulent normal stress in s-direction
τ	Shearing stress
τ_w	Wall shearing stress
o	Subscript denoting zero pressure gradient

ABSTRACT

Analytical relations have been derived for calculating a developing two-dimensional turbulent boundary layer in a pressure gradient from two simultaneous differential equations: momentum and shape parameter. An entrainment method is used to obtain the shape parameter equation. Both equations incorporate the velocity similarity laws that provide a two-parameter velocity profile general enough to include any range of Reynolds numbers. The entrainment factor is based on the characteristics of equilibrium pressure gradients in a way which can accommodate the usual pressure gradients found in engineering applications. The method includes a newly formed wake-modification function for the similarity laws as well as added effects due to low Reynolds numbers.

The variation of momentum loss boundary-layer thickness, local skin friction, and local velocity profile may be calculated for the boundary layers on hydrofoils and two-dimensional appendages. The various formulations are shown to correlate well with available experimental data.

ADMINISTRATIVE INFORMATION

The work described in this report was authorized and funded by the Independent Research Program of the David W. Taylor Naval Ship Research and Development Center under Project ZR-023-0101, Work Unit 1-1541-002.

INTRODUCTION

Analytical prediction of turbulent boundary layers in pressure gradients for two-dimensional flows such as exist on foils or struts may be expeditiously accomplished by the so-called integral methods that involve ordinary instead of partial differential equations. Here the classical von Kármán momentum equation is usually accompanied by a differential equation for the streamwise variation of the shape parameter of the velocity profile. Such a shape-parameter differential equation may be obtained readily from the entrainment method originally introduced by Head.[1]

As developed by Head, a one-parameter relation is empirically correlated between the usual shape parameter and a newly defined entrainment shape parameter. Then another newly defined entrainment factor is empirically correlated with the shape parameter in a

[1] Head, M.R., "Entrainment in the Turbulent Boundary Layer," Aeronautical Research Council R&M (Sep 1958).

A complete listing of references are given on page 40.

one-parameter relationship. A two-parameter method was later developed by Head and Patel[2] based on the Thompson charts for a two-parameter velocity profile. The entrainment factor based on equilibrium pressure gradients is presented on graphs.

A two-parameter entrainment method based on *velocity similarity laws* has been presented by Granville[3] as part of a synoptic group of such integral methods. The entrainment factor is obtained from boundary layers in equilibrium pressure gradients. By being stated in terms of momentum thickness Reynolds number and shape parameter, the entrainment factor is decoupled directly from the pressure gradient and, hence, becomes more responsive to nonequilibrium pressure gradients.

Recently an improvement[4] has been developed for the law of the wake and thus in the analytical description of the similarity laws. It is now proposed to apply this modification to the entrainment method. In addition, the skin friction law to be used is to be based on the similarity laws directly instead of a previously used generalized version of the Ludwieg-Tillmann formula. This allows inclusion of roughness effects and drag-reducing polymer effects more readily. When the turbulent boundary layer is considered a distinct layer, a momentum equation and an entrainment equation may be derived from the governing Reynolds equations for turbulent flow without the usual thin boundary-layer considerations. The results are additional terms arising from cross-pressure variations and normal stress, turbulent fluctuations. These, however, are important usually only close to separation of the boundary layer.

Velocity similarity laws incorporating a modification to the law of the wake are used to obtain a two-parameter variation of entrainment shape parameter as a function of the usual shape parameter and the local Reynolds number based on momentum thickness. The velocity similarity laws are also used to obtain a variation of local skin friction with these same two parameters, even at low values of the Reynolds number.

As stated before, the entrainment factor is analytically derived from boundary layers in equilibrium pressure gradients from a two-parameter relation with shape parameter and local Reynolds numbers. This decouples the entrainment factors directly from the local pressure gradient and provides a response to the cumulative history of the developing boundary layer.

---

[2]Head, M.R. and V.C. Patel, "Improved Entrainment Method for Calculating Turbulent Boundary Layer Development," Aeronautical Research Council R&M 3643 (Mar 1968).

[3]Granville, P.S., "Integral Methods for Turbulent Boundary Layers in Pressure Gradients," Journal of Ship Research, Vol. 16, No. 3, pp. 191-204 (Sep 1972).

[4]Granville, P.S., "A Modified Law of the Wake for Turbulent Shear Flow," NSRDC Report 4639 (Sep 1975).

Hence, the entrainment factor based on equilibrium pressure gradients may be applied to nonequilibrium pressure gradients.

For convenience all the analytical relations required for calculating the development of the turbulent boundary and the associated velocity profiles are listed in the appendix.

TWO-DIMENSIONAL TURBULENT BOUNDARY LAYERS

COORDINATE SYSTEM

For the two-dimensional boundary layer on foils, the coordinate system is defined in terms of families of surfaces parallel to the foil surface separated by normal distance y. The other coordinate s is specified along the contour representing families of surfaces orthogonal to the foil parallel surfaces. The arc length s is measured in the stream direction from the forward stagnation point while the normal distance y is measured outward from the foil surface.

EQUATIONS OF MOTION

For turbulent flow, the Reynolds equations, which are the averaged Navier-Stokes equations for laminar flow, are applied to the boundary-layer region. For the foil coordinate system and with the usual neglect of terms involving longitudinal curvature, the Reynolds equations of motion are in the s-direction.[5]

$$u \frac{\partial u}{\partial s} + v \frac{\partial u}{\partial y} = -\frac{1}{\rho} \frac{\partial p}{\partial s} + \frac{1}{\rho} \frac{\partial \tau}{\partial y} - \frac{1}{\rho} \frac{\partial \sigma_t}{\partial s} \tag{1}$$

and in the y-direction

$$u \frac{\partial v}{\partial s} + u \frac{\partial v}{\partial y} = -\frac{1}{\rho} \frac{\partial p}{\partial y} + \frac{1}{\rho} \frac{\partial \tau}{\partial s} - \frac{1}{\rho} \frac{\partial \tilde{\sigma}}{\partial y} \tag{2}$$

The equation of continuity is

$$\frac{\partial u}{\partial s} + \frac{\partial v}{\partial y} = 0 \tag{3}$$

[5] Schlichting, H., "Boundary-Layer Theory," Sixth Edition, McGraw-Hill Book Co., New York (1968).

where u = velocity in s-direction

v = velocity in y-direction

τ = shearing stress

σ_t = turbulent normal stress in s-direction

$\tilde{\sigma}$ = turbulent normal stress in y-direction

p = pressure

ρ = density of fluid

MOMENTUM EQUATION

The momentum equation results from an integration in the y-direction of Equation (1), of the s-equation of motion, and the inclusion of Equation (3), the equation of continuity

$$\frac{d\theta}{ds} + (H + 2)\frac{\theta}{U}\frac{dU}{ds} = \frac{\tau_w}{\rho U^2} + \frac{1}{\rho U^2}\frac{d}{ds}\int_o^\delta (p - p_\delta)\, dy + \frac{1}{\rho U^2}\frac{d}{ds}\int_o^\delta \sigma_t\, dy \qquad (4)$$

where θ = momentum thickness $= \int_o^\delta \left(1 - \frac{u}{U}\right)\frac{u}{U}\, dy$ (5)

δ = boundary-layer thickness

H = shape parameter $= \delta^*/\theta$ (6)

δ^* = displacement thickness $= \int_o^\delta \left(1 - \frac{u}{U}\right) dy$ (7)

τ_w = wall shearing stress

p_δ = pressure at outer edge of boundary layer

U = streamwise velocity at edge of boundary layer

This momentum equation differs from the classical von Kármán equation by the inclusion of the cross-pressure and normal-stress terms.

The momentum equation may also be conveniently written as

$$\frac{d\theta}{ds} + (H + 2)\frac{\theta}{U}\frac{dU}{ds} = \frac{\tau_w}{\rho U^2} + \frac{\hat{p}}{\rho U^2} + \frac{\hat{\sigma}}{\rho U^2} \qquad (8)$$

where

the cross-pressure term $\hat{p} = \frac{d}{ds}\int_o^\delta (p - p_\delta)\, dy$ (9)

and

the normal stress term $\hat{\sigma} = \frac{d}{ds}\int_o^\delta \sigma_t \, dy$. (10)

It should be noted that the cross-pressure and normal-stress terms become important usually only close to separation.

ENTRAINMENT EQUATION

The entrainment equation has been developed by Head[1] on the basis of physical arguments regarding the growth or entrainment of fluid in the developing turbulent boundary layer. It may also be obtained analytically by integrating the equation of continuity; see Equation (3).

$$\int_o^{\delta[s]} \frac{\partial u}{\partial s} \, dy + \int_o^{\delta[s]} \frac{\partial v}{\partial y} \, dy = 0 \tag{11}$$

which by the Leibnitz rule, and the boundary condition $v = 0$ at $y = 0$, gives

$$\frac{d}{ds}\int_o^\delta u \, dy - U\frac{d\delta}{ds} + v_\delta = 0 \tag{12}$$

where $v_\delta = v$ at $y = \delta$, the entrainment velocity.

To determine the entrainment velocity v_δ, Equation (1), the equation of motion, is evaluated at $y = \delta$; then

$$U\left(\frac{\partial u}{\partial s}\right)_\delta + v_\delta\left(\frac{\partial u}{\partial y}\right)_\delta = -\frac{1}{\rho}\left(\frac{\partial p}{\partial s}\right)_\delta + \frac{1}{\rho}\left(\frac{\partial \tau}{\partial y}\right)_\delta - \frac{1}{\rho}\left(\frac{\partial \sigma_t}{\partial s}\right)_\delta \tag{13}$$

Since in general along a streamline

$$\frac{du}{ds} = \frac{\partial u}{\partial s} + \frac{\partial u}{\partial y}\frac{dy}{ds} \tag{14}$$

then at $y = \delta$

$$\left(\frac{\partial u}{\partial s}\right)_\delta = \frac{dU}{ds} - \left(\frac{\partial u}{\partial y}\right)_\delta \frac{d\delta}{ds} \tag{15}$$

Likewise,

$$\left(\frac{\partial \sigma_t}{\partial s}\right)_\delta = \left(\frac{d\,\sigma_t}{ds}\right)_\delta - \left(\frac{\partial \sigma_t}{\partial y}\right)_\delta \frac{d\delta}{ds} \tag{16}$$

and

$$\left(\frac{\partial p}{\partial s}\right)_\delta = -\rho U \frac{dU}{ds} - \left(\frac{\partial p}{\partial y}\right)_\delta \frac{d\delta}{ds} \tag{17}$$

which follows from the Bernoulli theorem

$$\left(\frac{dp}{ds}\right)_\delta + \rho U \frac{dU}{ds} = 0 \tag{18}$$

With the foregoing and since $(\sigma_t)_\delta = 0$, the entrainment velocity v_δ in Equation (13) becomes

$$v_\delta = U \frac{d\delta}{ds} + \frac{1}{\rho}\left(\frac{\partial \tau}{\partial u}\right)_\delta + \frac{1}{\rho}\left[\frac{\partial (p + \sigma_t)}{\partial u}\right]_\delta \frac{d\delta}{ds} \tag{19}$$

Then Equation (12), the entrainment equation, is converted by means of Equation (19) to

$$\frac{d}{ds}\int_0^\delta u\, dy = UE \tag{20}$$

where

$$E = -\frac{1}{\rho U}\left(\frac{\partial \tau}{\partial u}\right)_\delta - \frac{1}{\rho U}\left[\frac{\partial (p + \sigma_t)}{\partial u}\right]_\delta \frac{d\delta}{ds} \tag{21}$$

is the entrainment factor. Also from the previous definitions, the entrainment equation may be written as

$$\frac{d}{ds}\left[U(\delta - \delta^*)\right] = UE \tag{22}$$

VELOCITY SIMILARITY LAWS

The velocity profile for turbulent boundary layers in pressure gradients may be specified by the classical velocity similarity laws which imply a two-parameter system. Correlation with experimental data has been well-established.[5]

For the usual moderate pressure gradient, the inner law or law of the wall of *smooth* flat plates (zero pressure gradient) has proved applicable which is stated in nondimensional ratios as

$$\frac{u}{u_\tau} = f[y^*] \tag{23}$$

where u = streamwise velocity component

u_τ = shear velocity

$$u_\tau = \sqrt{\tau_w/\rho} \tag{24}$$

τ_w = wall shearing stress

$$y^* = \frac{u_\tau y}{\nu} \tag{25}$$

ν = kinematic viscosity of fluid.

The inner law may be extended to include roughness effects[6] and drag-reducing effects of polymer solutions.[7]

For pressure gradients, the outer law or velocity-defect law may be stated as

$$\frac{U - u}{u_\tau} = f\left[\frac{y}{\delta}, B_2\right] \tag{26}$$

where B_2 is a velocity-defect factor that varies mostly with pressure gradient. Roughness effects or drag-reducing polymer effects do not affect the outer law.

Within the boundary layer, the two similarity laws may be considered to overlap which by the classical Millikan analysis leads to logarithmic functions within the overlapping region[3]; see Figure 1.

$$\frac{u}{u_\tau} = A \ln y^* + B_1 \qquad y_o^* \leqslant y^* \leqslant \left(\frac{y}{\delta}\right)_1 \eta \tag{27}$$

or

$$\frac{U - u}{u_\tau} = -A \ln \frac{y}{\delta} + B_2 \qquad \frac{y_o^*}{\eta} \leqslant \frac{y}{\delta} \leqslant \left(\frac{y}{\delta}\right)_1 \tag{28}$$

where A = constant

B_1 = the law-of-the-wall factor, which is constant for smooth surfaces and a variable for rough surfaces and drag-reducing polymer solutions[6,7]

[6] Granville, P.S., "The Frictional Resistance and Turbulent Boundary Layer of Rough Surfaces," Journal of Ship Research, Vol. 2, No. 3, pp. 52-74 (Dec 1958).

[7] Granville, P.S., "The Frictional Resistance and Velocity Similarity Laws of Drag-Reducing Polymer Solutions," Journal of Ship Research, Vol. 12, No. 3, pp. 201-212 (Sep 1968).

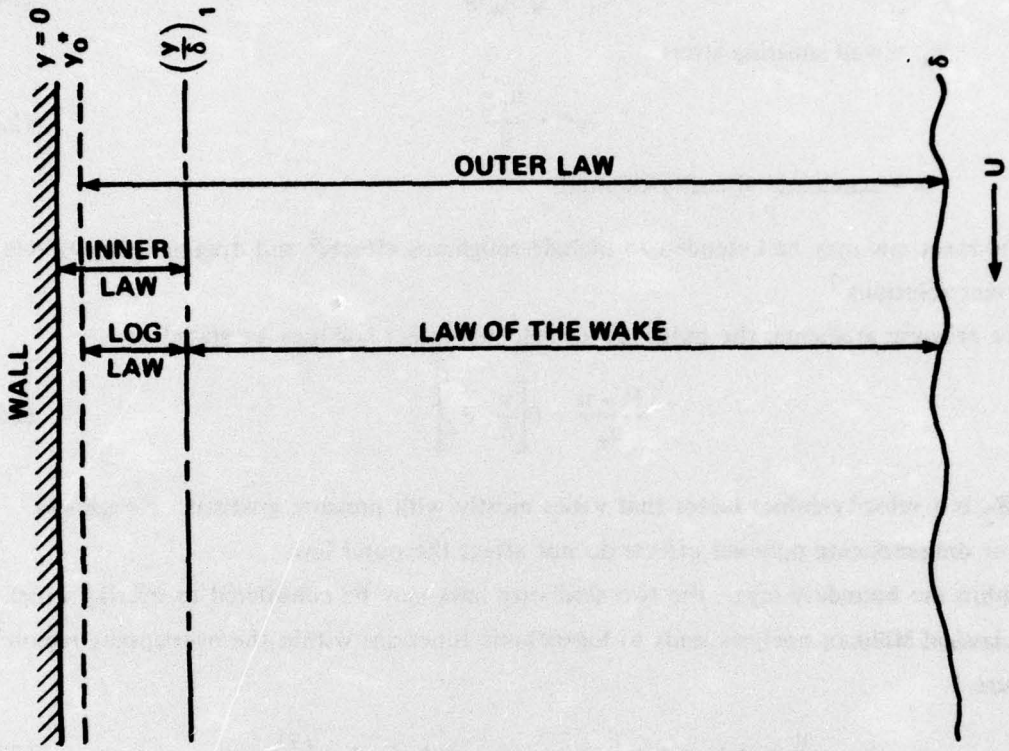

VELOCITY PROFILES

INNER LAW $\frac{u}{u_\tau} = f[y^*], \qquad 0 \le y^* \le \eta\left(\frac{y}{\delta}\right)_1$

LOG LAW $\frac{u}{u_\tau} = A \ln y^* + B_1, \qquad y_o^* \le y^* \le \eta\left(\frac{y}{\delta}\right)_1$

OUTER LAW $\frac{u}{u_\tau} = A \ln y^* + B_1 + B_2 \frac{w}{2}\left[\frac{y}{\delta}\right] + Aq\left[\frac{y}{\delta}\right], \; y_o^* \le y^* \le \eta$

Figure 1 – Velocity Similarity Laws for Turbulent Boundary Layers

$$\eta = \frac{u_\tau \delta}{\nu} \tag{29}$$

y_o^* = inner limit of log law

$\left(\frac{y}{\delta}\right)_1$ = outer limit of log law

The region in the boundary layer *outside* the logarithmic region has been fitted by the Coles law of the wake, which in subsequent modification[4] may be included with the log law for the range $y_o^* \leq y^* \leq \eta$

$$\frac{u}{u_\tau} = A \ln y^* + B_1 + B_2 \frac{w}{2}\left[\frac{y}{\delta}\right] + A\, q\left[\frac{y}{\delta}\right] \tag{30a}$$

or for the range $\frac{y_o^*}{\eta} \leq \frac{y}{\delta} \leq 1$

$$\frac{U - u}{u_\tau} = - A \ln \frac{y}{\delta} + B_2 - B_2 \frac{w}{2}\left[\frac{y}{\delta}\right] - A\, q\left[\frac{y}{\delta}\right] \tag{30b}$$

where w is a wake function, and q is a wake-modification function.

Moses[4] gives a polynomial expression for w

$$\frac{w}{2} = 3\left(\frac{y}{\delta}\right)^2 - 2\left(\frac{y}{\delta}\right)^3 \tag{31}$$

and Granville[4] for q

$$q = \left(\frac{y}{\delta}\right)^2 \left(1 - \frac{y}{\delta}\right) \tag{32}$$

For convenience w and q are considered to start at the wall y = 0.

BOUNDARY-LAYER PARAMETERS

Boundary-layer parameters suggested by the outer similarity law are

$$I_1 = \int_0^1 \left(\frac{U - u}{u_\tau}\right) d\left[\frac{y}{\delta}\right] \tag{33}$$

which from definitions results in

$$I_1 = \sigma\left(\frac{\delta^*}{\delta}\right) \tag{34}$$

where $\sigma = \frac{U}{u_\tau} = \left(\frac{\tau_w}{\rho U^2}\right)^{-1/2}$ is a local skin-friction coefficient, (35)

and

$$I_2 = \int_0^1 \left(\frac{U - u}{u_\tau}\right)^2 d\left[\frac{y}{\delta}\right] \tag{36}$$

which from definitions results in

$$I_2 = \sigma^2 \left(\frac{\delta^*}{\delta} - \frac{\theta}{\delta}\right) \tag{37}$$

The Rotta-Clauser shape parameter G defined by

$$G = I_2/I_1 \tag{38}$$

becomes from previous definitions

$$G = \sigma \left(1 - \frac{1}{H}\right) \tag{39}$$

This relation for G is independent of the choice of velocity profile.

If the similarity laws as expressed by Equations (27) and (30) are used to evaluate I_1 and I_2, then

$$I_1 = \frac{11}{12} A + \frac{1}{2} B_2 + \frac{\lambda_1}{\eta} \tag{40}$$

and

$$I_2 = \frac{4819}{2520} A^2 + \frac{213}{140} A B_2 + \frac{13}{35} B_2^2 + \frac{2\lambda_1 \sigma - \lambda_2}{\eta} \tag{41}$$

where

$$\lambda_1 = (A \ln y_o^* + B_1 - A) y_o^* - \int_o^{y_o^*} \frac{u}{u_\tau} dy^* \tag{42}$$

and

$$\lambda_2 = [(A \ln y_o^* + B_1)^2 - 2A(A \ln y_o^* + B_1) + 2A^2] y_o^* - \int_o^{y_o^*} \left(\frac{u}{u_\tau}\right)^2 dy^* \tag{43}$$

For very high values of Reynolds numbers, η becomes increasingly larger; hence, the λ-terms may be neglected. Then

$$I_1 = \frac{11}{12} A + \frac{1}{2} B_2 \tag{44}$$

and

$$I_2 = \frac{4819}{2520} A^2 + \frac{213}{140} A B_2 + \frac{13}{35} B_2^2 \tag{45}$$

The same results are obtained if the outer law is assumed to hold all the way to the wall $y = 0$.

ENTRAINMENT SHAPE PARAMETER

The entrainment thickness is defined as the difference $\delta - \delta^*$ and the entrainment shape parameter $\tilde{H}$ is defined as the ratio

$$\tilde{H} = \frac{\delta - \delta^*}{\theta} = \frac{\delta}{\theta} - H \tag{46}$$

For one-parameter velocity profiles,

$$\tilde{H} = f[H]$$

and for two-parameter velocity profiles,

$$\tilde{H} = f[H, R_\theta]$$

where

$$R_\theta = \frac{U\theta}{\nu} \tag{47}$$

ONE-PARAMETER RELATIONS

The power-law velocity profile

$$\frac{u}{U} = \left(\frac{y}{\delta}\right)^n \tag{48}$$

gives

$$\tilde{H} = \frac{2H}{H - 1} \tag{49}$$

and

$$\frac{d\tilde{H}}{dH} = -\frac{2}{(H - 1)^2} \tag{50}$$

An empirical fit to airfoil data for $1.4 \times 10^3 < R_\theta < 7.6 \times 10^4$ by Head[8] yields another one-parameter relation

$$\tilde{H} = 1.535\,(H - 0.7)^{-2.715} + 3.3 \tag{51}$$

and

$$\frac{d\tilde{H}}{dH} = -4.168\,(H - 0.7)^{-3.715} \tag{52}$$

TWO-PARAMETER RELATIONS

The similarity laws provide a two-parameter relation for the entrainment shape parameter. From Equations (34) and (39)

$$\frac{\theta}{\delta} = \frac{I_1}{\sigma}\left(1 - \frac{G}{\sigma}\right) \tag{53}$$

and with Equation (39)

$$\frac{\theta}{\delta} = \frac{I_1}{G}\left(\frac{H - 1}{H}\right) \tag{54}$$

Then from Equation (46)

$$\tilde{H} = \left(\frac{G}{I_1}\right)\left(\frac{H^2}{H - 1}\right) - H \tag{55}$$

This equation has been also obtained by Michel, Quemard, and Durant.[8]

G/I_1 may be related to G through Equations (44) and (45) with B_2 as the implicit parameter. At separation $B_2 \to \infty$ and $G/I_1 \to 1.4857$. A close fit is given numerically by

$$\frac{G}{I_1} = 1.4857 + \frac{0.4739\,A}{G} + \frac{5\,A^2}{G^{2.75}} \tag{56}$$

Then the entrainment shape parameter becomes

$$\tilde{H} = \left(\frac{H^2}{H - 1}\right)\left(1.4857 + \frac{0.4739\,A}{G} + \frac{5\,A^2}{G^{2.75}}\right) - H \tag{57}$$

where G is a function of H and R_θ through Equation (39). Then,

[8] "Proceedings–Computation of Turbulent Boundary Layers, 1968 AFOSR-IFP Stanford Conference," Edited by Kline, S.J. et al., Vol. 1, Thermosciences Division, Stanford University (1968).

$$\frac{\partial \tilde{H}}{\partial H} = \frac{H(H-2)-H}{H(H-1)} - \left(\frac{H^2}{H-1}\right)\left(\frac{0.4739\,A}{G} + \frac{13.75\,A^2}{G^{2.75}}\right)\left[\frac{1}{H(H-1)} + \frac{\partial \ln \sigma}{\partial H}\right] \tag{58}$$

and

$$\frac{\partial \tilde{H}}{\partial \ln R_\theta} = -\left(\frac{H^2}{H-1}\right)\left(\frac{0.4739\,A}{G} + \frac{13.75\,A^2}{G^{2.75}}\right)\frac{\partial \ln \sigma}{\partial \ln R_\theta} \tag{59}$$

LOCAL SKIN FRICTION

The similarity laws not only specify the velocity profile but also the local skin friction. From the logarithmic forms of the inner and outer similarity laws, Equations (27) and (28)

$$\sigma = A \ln y + B_1 + B_2 \tag{60}$$

The objective now is to determine σ as a function of local Reynolds number R_θ and shape parameter H.

Equation (60) is rewritten as

$$\sigma = A \ln\left[\frac{1}{\sigma}\left(\frac{\delta}{\theta}\right) R_\theta\right] + B_1 + B_2 \tag{61}$$

Since from Equation (34)

$$\frac{\theta}{\delta} = \frac{I_1}{\sigma H} \tag{62}$$

and from Equation (44)

$$B_2 = 2I_1 - \frac{11}{6} A \tag{63}$$

$$\sigma = A \ln H R_\theta + B_1 - \frac{11}{6} A + 2I_1 - A \ln I_1 \tag{64}$$

I_1 is a function of G from Equations (44) and (45). An empirical fit is given by

$$2I_1 - A \ln I_1 = 1.3462\,G - 0.2605\,A - 0.9392\,A \ln G \tag{65}$$

Then G is a function of σ and H in Equation (39) which leads to

$$\frac{0.3462(3.889 - H)}{H}\sigma + 0.9392\,A \ln \sigma = A \ln R_\theta + B_1 - 2.0938\,A - A \ln\left[\frac{(H-1)^{0.9392}}{H^{1.9392}}\right] \tag{66}$$

This is the *implicit* relation for local skin friction coefficient σ as a function of R_θ and H. The factor B_1 is a constant for smooth surfaces and a variable for rough surfaces and/or drag-reducing polymers. At separation $\sigma \to \infty$, $H \to 3.889$.

An approximate *explicit* expression may be obtained which is accurate, except near separation. A numerical fit gives

$$2 I_1 - A \ln I_1 = 1.167 G - 1.577 A \tag{67}$$

Then

$$\sigma = \left(\frac{H}{1.167 - 0.167 H}\right)(A \ln H R_\theta + B_1 - 3.410 A) \tag{68}$$

The approximate value of σ may be used to obtain a more accurate value by reiteration. If

$$\sigma = \bar{\sigma} + \epsilon \tag{69}$$

where $\bar{\sigma}$ = approximate value of σ

ϵ = correction of σ

then by infinitesimal analysis of Equation (66)

$$\epsilon = \frac{\gamma - \alpha \bar{\sigma} - \bar{\beta} \ln \sigma}{\alpha + \frac{\bar{\beta}}{\sigma}} \tag{70}$$

where

$$\alpha = \frac{0.3462 (3.889 - H)}{H} \tag{71}$$

$$\bar{\beta} = 0.9392 A \tag{72}$$

and

$$\gamma = A \ln R_\theta + B_1 - 2.0938 A - A \ln \left[\frac{(H - 1)^{0.9392}}{H^{1.9392}}\right] \tag{73}$$

Partial derivatives of skin friction parameter σ required in the subsequent analysis may be obtained from Equation (66)

$$\frac{\partial \ln \sigma}{\partial H} = \frac{2.8885}{H(H - 1)} \left[\frac{1.3462(H - 1)\sigma + A H(H - 1.9392)}{(3.889 - H)\sigma + 2.7129 A H}\right] \tag{74}$$

and

$$\frac{\partial \ln \sigma}{\partial \ln R_\theta} = \frac{2.8885\, A\, H}{(3.889 - H)\sigma + 2.7129\, A\, H} \tag{75}$$

EQUILIBRIUM PRESSURE GRADIENTS

PRESSURE-GRADIENT PARAMETER

Similarity is maintained in the velocity-defect law if the Clauser pressure-gradient parameter[3]

$$\beta = \frac{\delta^*}{\tau_w}\frac{dp}{ds} = -H\sigma^2\frac{\theta}{U}\frac{dU}{ds} \tag{76}$$

is maintained constant with respect to s or $d\beta/ds = 0$. This is the condition for an equilibrium pressure gradient; B_2 is constant, and, for the most part, G is constant.

It has been found empirically[3] that for equilibrium pressure gradients $\tilde{G}$ is a function of β so that

$$\tilde{G} = a_1\sqrt{a_2 + \beta} - a_3 \tag{77}$$

where a_1, a_2, and a_3 are constants.

SHAPE PARAMETER EQUATION

The local skin friction coefficient σ is given by

$$\sigma = A \ln H R_\theta + B_1 - \frac{11}{6}A + 2I_1 - A \ln I_1 \tag{64}$$

From Equation (39)

$$\frac{H}{H-1} = \frac{G}{\sigma} = \frac{A}{G}\ln H R_\theta + \frac{B_1}{G} - \frac{11}{6}\frac{A}{G} + \frac{2I_1}{G} - \frac{A}{G} I_1 \tag{78}$$

where A is in general a constant, and B_1 is a constant for smooth surfaces.

For equilibrium pressure gradients, G and I_1 are constant with respect to s. By differentiation of Equation (78)

$$\theta\frac{dH}{ds} = -\left[\frac{A\,H(H-1)^2}{A(H-1)^2 + GH}\right]\theta\frac{d\ln R_\theta}{ds} \tag{79}$$

for equilibrium pressure gradients.

SHAPE PARAMETER DIFFERENTIAL EQUATION

The entrainment equation Equation (22) is converted into a differential equation for shape parameter (dH/ds) as follows. In terms of entrainment shape parameter, $\tilde{H} = (\delta - \delta^*)/\theta$

$$\theta \frac{d\tilde{H}}{ds} = E - \tilde{H} \frac{d\theta}{ds} - \tilde{H} \frac{\theta}{U} \frac{dU}{ds} \tag{80}$$

or

$$\theta \frac{d\tilde{H}}{ds} = E - \tilde{H}\theta \frac{d \ln R_\theta}{ds} \tag{81}$$

Now for two-parameter velocity profiles

$$\tilde{H} = f[H, \ln R_\theta] \tag{82}$$

Equation (82) when expanded into partial derivatives becomes

$$\frac{d\tilde{H}}{ds} = \left(\frac{\partial \tilde{H}}{\partial H}\right)\frac{dH}{ds} + \left(\frac{\partial \tilde{H}}{\partial \ln R_\theta}\right)\frac{d \ln R_\theta}{ds} \tag{83}$$

Then

$$\theta \frac{dH}{ds} = \left(\frac{\partial H}{\partial \tilde{H}}\right)E - \left(\frac{\partial H}{\partial \tilde{H}}\right)\left(\tilde{H} + \frac{\partial \tilde{H}}{\partial \ln R_\theta}\right)\theta \frac{d \ln R_\theta}{ds} \tag{84}$$

From the momentum equation Equation (8)

$$\theta \frac{d \ln R_\theta}{ds} = \frac{1}{\sigma^2} + \frac{\hat{p} + \hat{\sigma}}{\rho U^2} - (H + 1)\frac{\theta}{U}\frac{dU}{ds} \tag{85}$$

Finally

$$\theta \frac{dH}{ds} = (H + 1)\left[\tilde{H} + \left(\frac{\partial \tilde{H}}{\partial \ln R_\theta}\right)\right]\left(\frac{\partial H}{\partial \tilde{H}}\right)\frac{\theta}{U}\frac{dU}{ds} - \left[\tilde{H} + \left(\frac{\partial \tilde{H}}{\partial \ln R_\theta}\right)\right]\left(\frac{\partial H}{\partial \tilde{H}}\right)\frac{1}{\sigma^2}$$

$$+ E\left(\frac{\partial H}{\partial \tilde{H}}\right) - \left[\tilde{H} + \left(\frac{\partial \tilde{H}}{\partial \ln R_\theta}\right)\right]\left(\frac{\partial H}{\partial \tilde{H}}\right)\frac{(\hat{p} + \hat{\sigma})}{\rho U^2} \tag{86}$$

or

$$\theta \frac{dH}{ds} = -M\frac{\theta}{U}\frac{dU}{ds} + \frac{M}{(H + 1)}\frac{1}{\sigma^2} - E\left(-\frac{\partial H}{\partial \tilde{H}}\right) + \frac{M}{(H + 1)}\frac{(\hat{p} + \hat{\sigma})}{\rho U^2} \tag{87}$$

where

$$M = (H + 1)\left[\tilde{H} + \left(\frac{\partial \tilde{H}}{\partial \ln R_\theta}\right)\right]\left(-\frac{\partial H}{\partial \tilde{H}}\right) \tag{88}$$

is a pressure-gradient factor; M represents the ability of the shape parameter differential equation to respond to external pressure gradients.

ENTRAINMENT FACTOR

For equilibrium pressure gradients, the entrainment factor designated as "E_e" is obtained from Equations (72) and (78)

$$E_e = \left\{\tilde{H} + \left(\frac{\partial \tilde{H}}{\partial \ln R_\theta}\right) - \left(\frac{\partial \tilde{H}}{\partial H}\right)\left[\frac{A\,H(H-1)^2}{A(H-1)^2 + G\,H}\right]\right\}\theta\,\frac{d \ln R_\theta}{ds} \tag{89}$$

or, from Equations (76) and (85)

$$E_e = \left\{\tilde{H} + \left(\frac{\partial \tilde{H}}{\partial \ln R_\theta}\right) - \left(\frac{\partial \tilde{H}}{\partial H}\right)\left[\frac{A\,H(H-1)^2}{A(H-1)^2 + G\,H}\right]\right\}\left\{\left[1 + \frac{(H+1)}{H}\beta\right]\frac{1}{\sigma^2} + \frac{(\hat{p} + \hat{\sigma})}{\rho U^2}\right\} \tag{90}$$

where E_e is a function of H and R_θ, since β depends on G in Equation (77), and G and σ are functions of H and R_θ from Equations (39) and (66).

EFFECT OF LOW REYNOLDS NUMBER

For smooth flat plates (zero pressure gradient), it has been found[9] that the velocity-defect factor B_2, instead of being constant, is a function of local skin-friction coefficient σ for low values of σ. This may be stated as

$$B_2 = \tilde{B}_2[0] - \Delta B[\sigma] \tag{91}$$

$\tilde{B}_2$ is the part of B_2 affected by pressure-gradient parameter β and ΔB_2 by low Reynolds number. Since G from Equations (38), (40), and (41) is a function of B_2, then

$$G = \tilde{G}[0] - \Delta G[\sigma] \tag{92}$$

$\tilde{G}$ is the part of G affected by pressure-gradient β and ΔG by low Reynolds number.

[9] Granville, P.S., "The Drag and Turbulent Boundary Layer of Flat Plates at Low Reynolds Numbers," DTNSRDC Report 4682 (Dec 1975).

As shown by Cebeci and Mosinskis,[10] a low Reynolds number effect exists also for pressure gradients. For a pressure gradient these relations may be generalized to

$$B_2 = \tilde{B}_2 [\beta] - \Delta B[\sigma] \tag{93}$$

and

$$G = \tilde{G}[\beta] - \Delta G[\sigma] \tag{94}$$

Equation (77) also becomes

$$\tilde{G}[\beta] = a_1 \sqrt{a_2 + \beta} - a_3 \tag{95}$$

INITIAL CONDITIONS AT TRANSITION

At the transition point from laminar to turbulent flow, there is physically no change in momentum loss since such a loss would require an impulsive force. Then at transition

$$(R_\theta)_{turb} = (R_\theta)_{lam} \tag{96}$$

If turbulence stimulation of some kind were to be used to hasten transition, then an additional momentum loss, expressed as ΔR_θ, would arise as a result of the separation drag of the stimulator. Then at transition

$$(R_\theta)_{turb} = (R_\theta)_{lam} + \Delta R_\theta \tag{97}$$

The problem of an initial value of shape parameter H at transition is more difficult. During transition the high values of H in laminar flow undergo a rapid decrease to the lower values of H in turbulent flow. For pressure gradients, no method of predicting an initial value of H seems to exist. Instead, a convenient initial value of H is that of $H_o[R_\theta]$ for zero pressure gradient.

For zero pressure gradient, from Equation (39)

$$\frac{1}{H_o} = 1 - \frac{G_o}{\sigma_o} \tag{98}$$

or for the low Reynolds number effect of Equation (90)

[10] Cebeci, T. and G.J. Mosinskis, "Computation of Incompressible Turbulent Boundary Layers at Low Reynolds Numbers," American Institute of Aeronautics and Astronautics Journal, Vol. 9, No. 8, pp. 1632-1634 (Aug 1971).

$$\frac{1}{H_o} = 1 - \frac{(\tilde{G}_o - \Delta G[\sigma_o])}{\sigma_o} \tag{99}$$

Also as shown in Reference 3

$$\sigma_o = \alpha_1 \ln R_\theta + \alpha_2 \tag{100}$$

The subscript o refers to conditions at zero pressure gradient.

NUMERICAL EVALUATIONS

Although analytical expressions have been developed for the relationships needed to determine the development of two-dimensional turbulent boundary layers, there remain constants whose values have to be supplied empirically.

Numerical comparisons of the various properties of the velocity profile are to be made for different values of shape parameter H and Reynolds number R_θ which represent the two-parameter characterization. The value of $R_\theta = 10^4$ used is representative of laboratory conditions, while the value of $R_\theta = 10^6$ is representative of boundary layers found in many underwater applications. The values of H range from 1.4 representative of flat-plate conditions to 3, representing a high value for separation. On airfoils, separation may occur for a value of H from 1.8 to 2.6.

SIMILARITY-LAW CONSTANTS

Values of $B_1 = 3.88$ and $A = 2.606$ have been found[9] to give flat-plate drag results close to the well-accepted Schoenherr line at high Reynolds numbers. These values are used in the following numerical evaluations.

LOCAL SKIN FRICTION

Values of local skin-friction coefficient $\tau_w/(\rho U^2)$ obtained from the similarity-law solution in Equation (66) are shown in Figure 2 as a function of shape parameter H for fixed values of $R_\theta = 10^4$ and 10^6. There is the expected decrease in the local skin-friction coefficient with increasing H, representative of adverse pressure gradients, and with increasing R_θ, representative of a thickening boundary layer.

A comparison with the Ludwieg-Tillmann[3] formula is also shown

$$\frac{\tau_w}{\rho U^2} = \frac{0.123}{e^{1.561\,H}\, R_\theta^{0.268}} \tag{101}$$

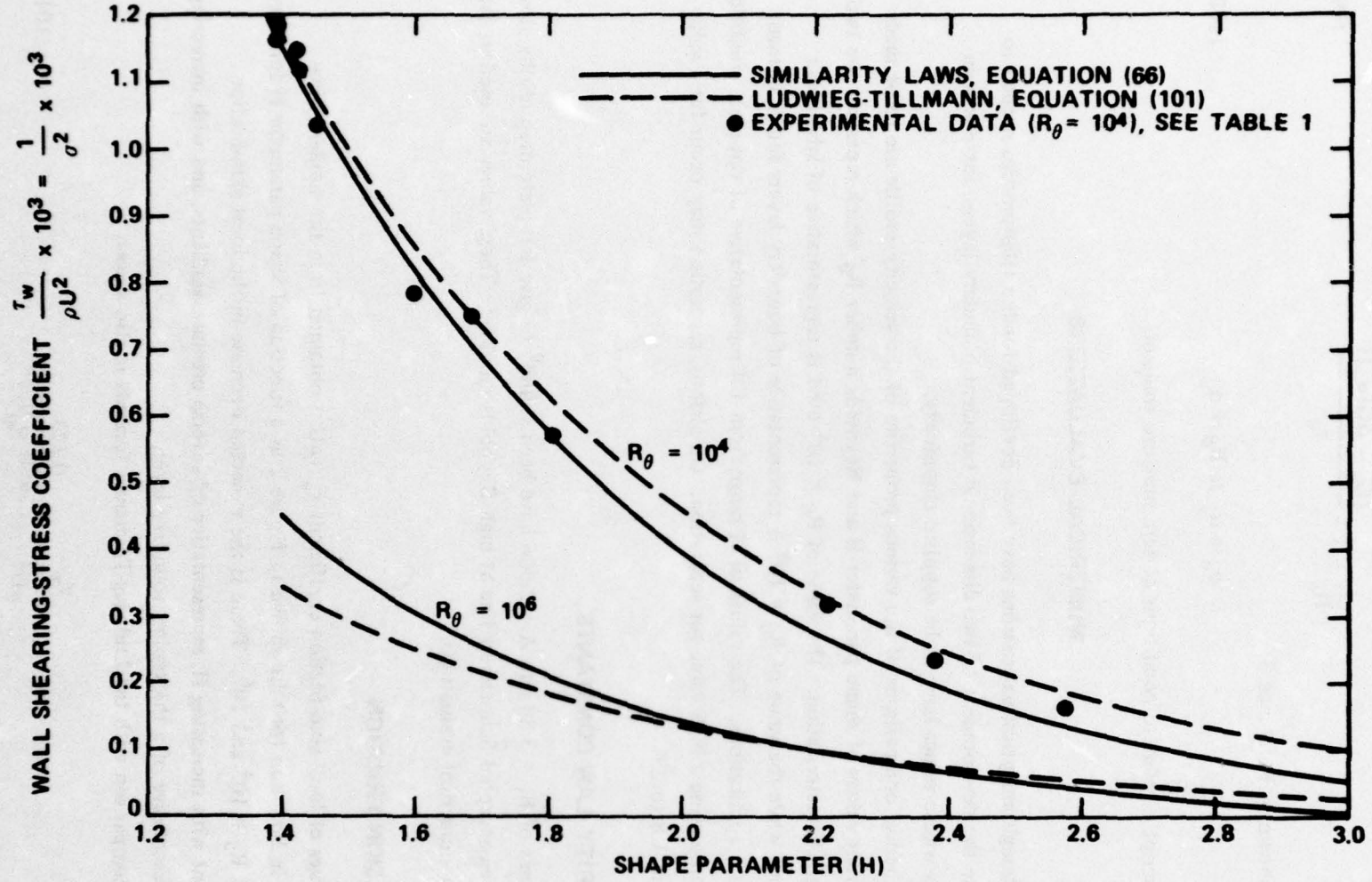

Figure 2 – Wall Shearing-Stress Coefficient

The Ludwieg-Tillman formula represents an empirical fit to data around $R_\theta = 10^4$ and is unreliable for $R_\theta = 10^6$.

Also shown are test data[11] at $R_\theta = 10^4$ for a variety of boundary layers which are listed in Table 1. There is good agreement between the test data, the similarity law formula, and the Ludwieg-Tillmann formula. Unfortunately there do not seem to be test data for $R_\theta = 10^6$.

TABLE 1 – BOUNDARY-LAYER DATA FOR $R_\theta = 10^4$

(Obtained by interpolation of values listed in Reference 11)

Flow No.	Description of Boundary-Layer Flow	$\frac{\tau_w}{\rho U^2} \times 10^3$	H	G	$\tilde{H}$
1100	Ludwieg and Tillmann, Mild Adverse Pressure Gradient	1.18	1.397	8.27	7.61
1200	Ludwieg and Tillmann, Strong Adverse Pressure Gradient	1.115	1.426	8.95	7.76
1500	Tillmann, Ledge Flow	1.445	1.283	5.80	8.74
2100	Schubauer and Klebanoff	1.265	1.353	7.34	8.18
2300	Clauser, Equilibrium Moderate Adverse Pressure Gradient	0.57	1.804	18.67	4.42
2500	Bradshaw, Equilibrium Mild Adverse Pressure Gradient	1.15	1.426	8.81	6.55
3500	Newman, Adverse Pressure Gradient	0.755	1.636	14.15	4.76
4400	Schubauer and Spangenberg, Strong Adverse Pressure Gradient	0.785	1.597	13.34	5.45
4500		1.0375	1.454	9.69	6.68
4800		1.16	1.395	8.31	7.05
5000	Fraser, Flow in Round Diffuser	0.23	2.372	38.14	4.65
5100		0.32	2.221	30.73	5.13
5300	Stratford, Nearly Separating Boundary Layer	0.164	2.573	47.74	3.75

Partial derivatives of σ, with respect to H and R_θ in Equations (74) and (75) needed in the analysis, are shown in Figures 3 and 4. In comparison, the results from the Ludwieg-Tillmann formula show constant values for $(\partial \ln \sigma)/\partial H$ and $(\partial \ln \sigma)/(\partial \ln R_\theta)$. Experimentally derived results are not plotted because they are not sufficiently precise to determine such derivatives.

[11] "Proceedings–Computation of Turbulent Boundary Layers, 1968 AFOSR-IFP Stanford Conference," Edited by Coles, D.E. and E.A. Hirst, Vol. 2, Thermosciences Division, Stanford University (1968).

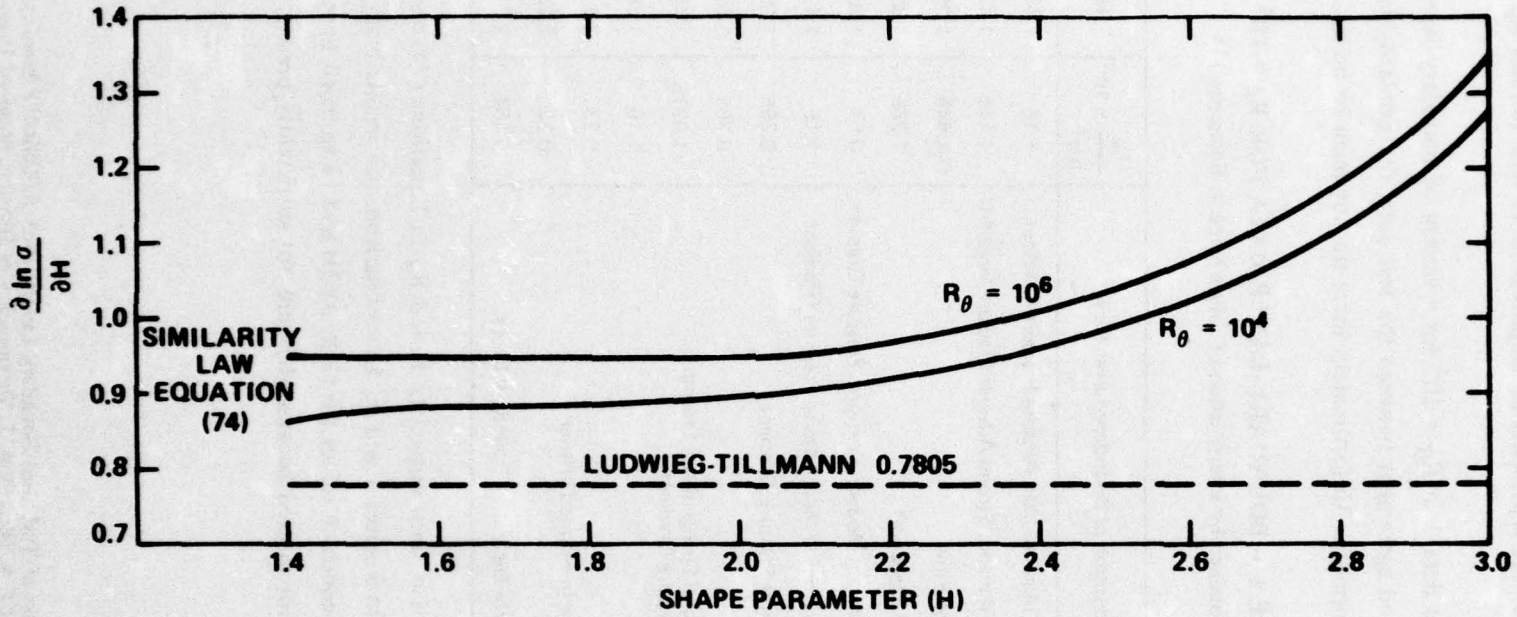

Figure 3 – Variation of $\partial \ln \sigma / \partial H$

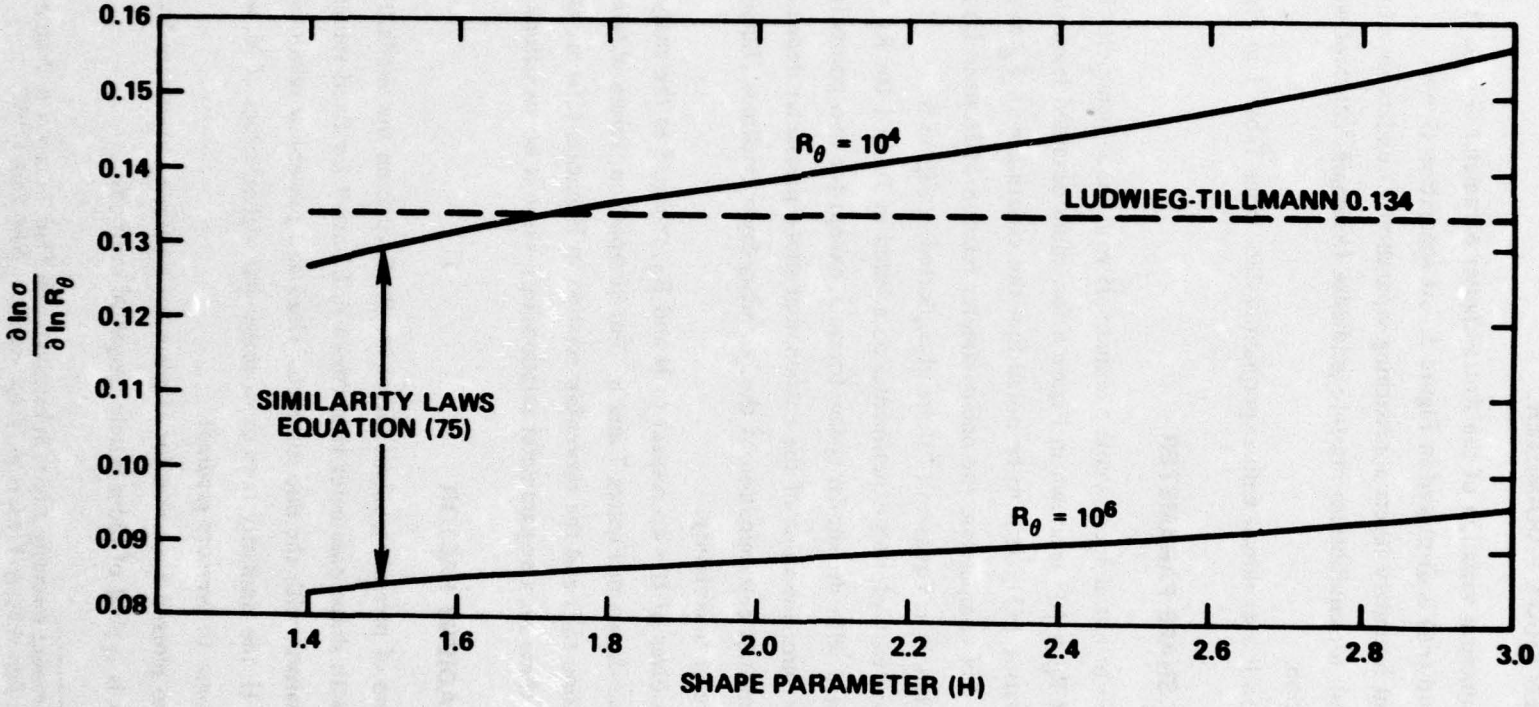

Figure 4 – Variation of $\partial \ln \sigma / \partial \ln R_\theta$

ROTTA-CLAUSER SHAPE PARAMETER

The large numerical variation of the Rotta-Clauser parameter G with H and R_θ from Equations (39) and (66) is displayed in Figure 5. At separation $G \to \infty$.

For turbulent boundary layers approaching separation, G undergoes a large variation. On the other hand, for equilibrium pressure gradients, G remains constant with respect to the streamwise direction.

A comparison is also shown with experimental data from Table 1 in Figure 5.

ENTRAINMENT SHAPE PARAMETER

The variation of entrainment shape parameter $\tilde{H}$ with shape parameter H at fixed values of $R_\theta = 10^4$ and $R_\theta = 10^6$ is shown in Figure 6 for values obtained from similarity-law formula; see Equation (57). It is to be noted that the variation with R_θ is greatest at the low values of H. For comparison, the one-parameter relation of Head in Equation (51) and the power-law relation in Equation (49) are also plotted in Figure 6.

A comparison with plotted experimental data listed in Table 1 for $R_\theta = 10^4$ shows excellent agreement with the similarity-law formula, except for two points from Fraser Flows 5000 and 5100. Since the value of the entrainment shape parameter depends on the very imprecise experimental determination of the boundary-layer thickness (Equation (46)) there is a large measure of uncertainty.

Partial derivatives of H with respect to H and R_θ, required in the analysis from Equations (58) and (59), are shown in Figures 7 and 8. For comparison, values obtained from the Head relation of Equation (52) and the power-law relation in Equation (50) are also shown in Figure 7. Since these are one-parameter relationships, there is no variations with R_θ.

PRESSURE-GRADIENT FACTOR

The variation of pressure-gradient factor M, obtained from the similarity laws of Equation (88), with shape parameter H is shown in Figure 9 for fixed values of $R_\theta = 10^4$ and 10^6. Comparison with the one-parameter Head and power-law relations is also given. At higher values of H, the similarity laws show somewhat higher values of M, which indicates a more rapid response to pressure gradient.

There is also plotted a relation for M given for separating boundary layers on airfoils by Garner,[12] which is typical of older purely empirical methods:

[12] Rotta, J.C., "Turbulent Boundary Layers in Incompressible Flow," Chapter in Progress in Aeronautical Sciences, Vol. 2, Edited by A. Ferri, et al., Pergamon Press, New York (1962).

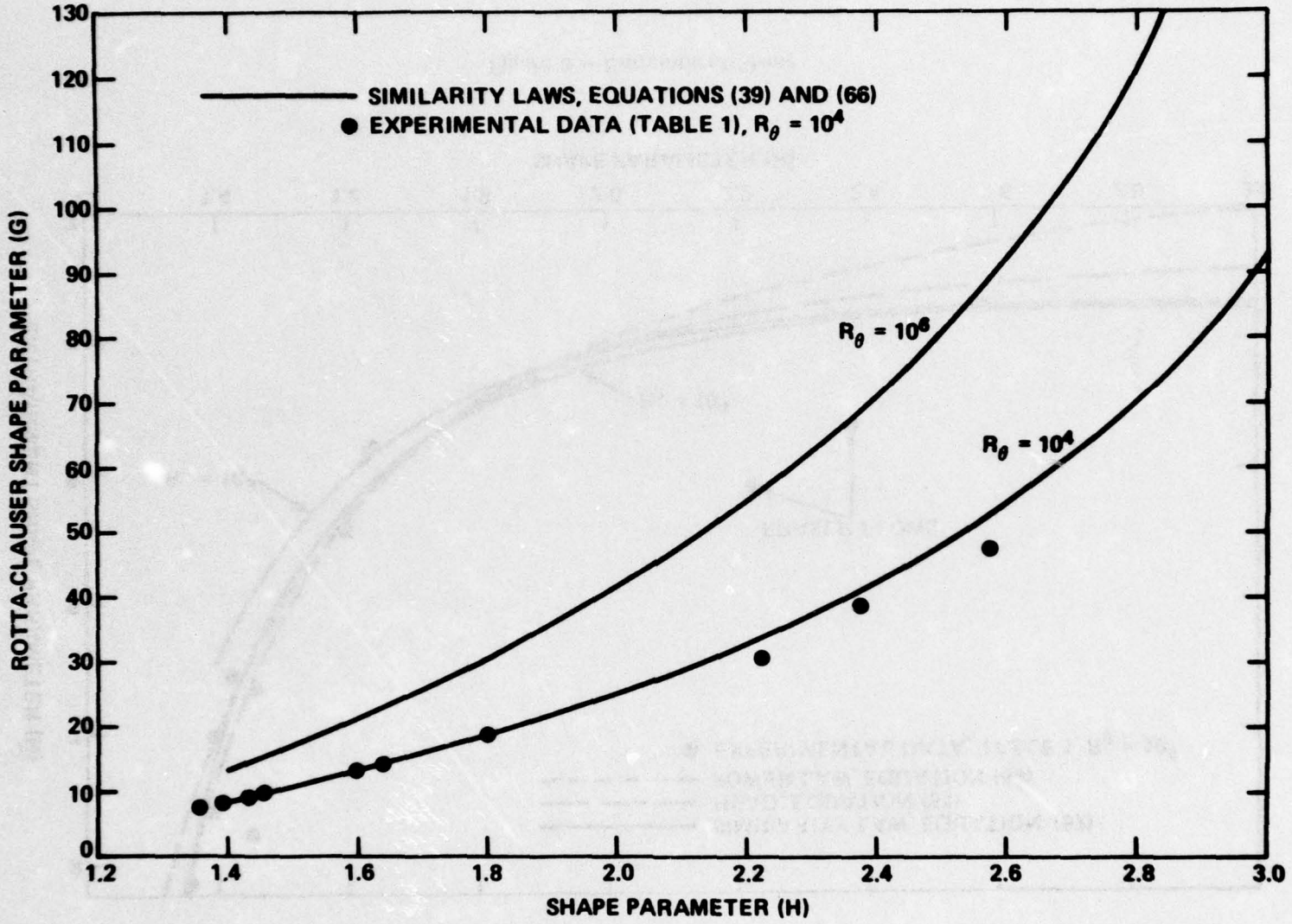

Figure 5 – Rotta-Clauser Shape Parameter

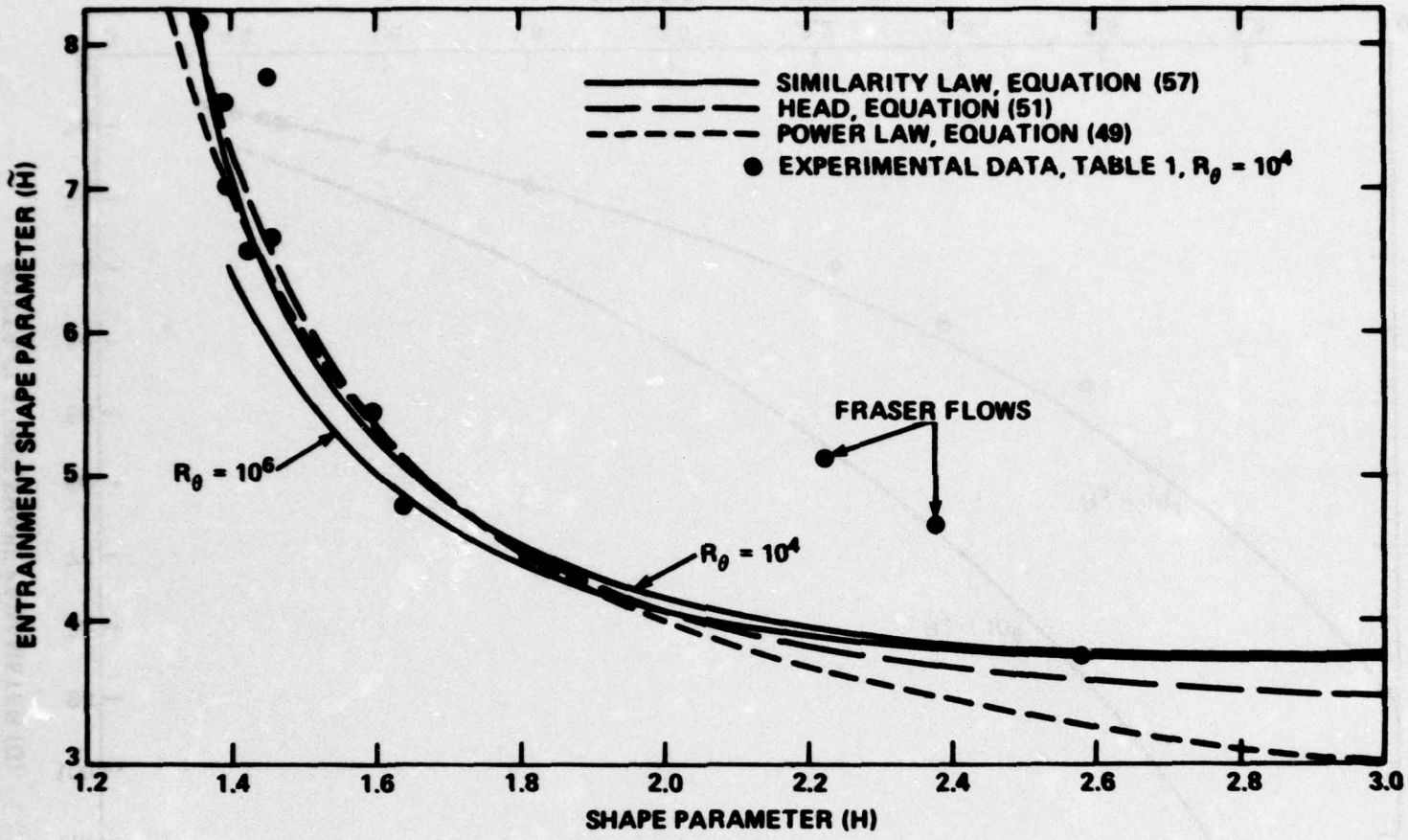

Figure 6 – Entrainment Shape

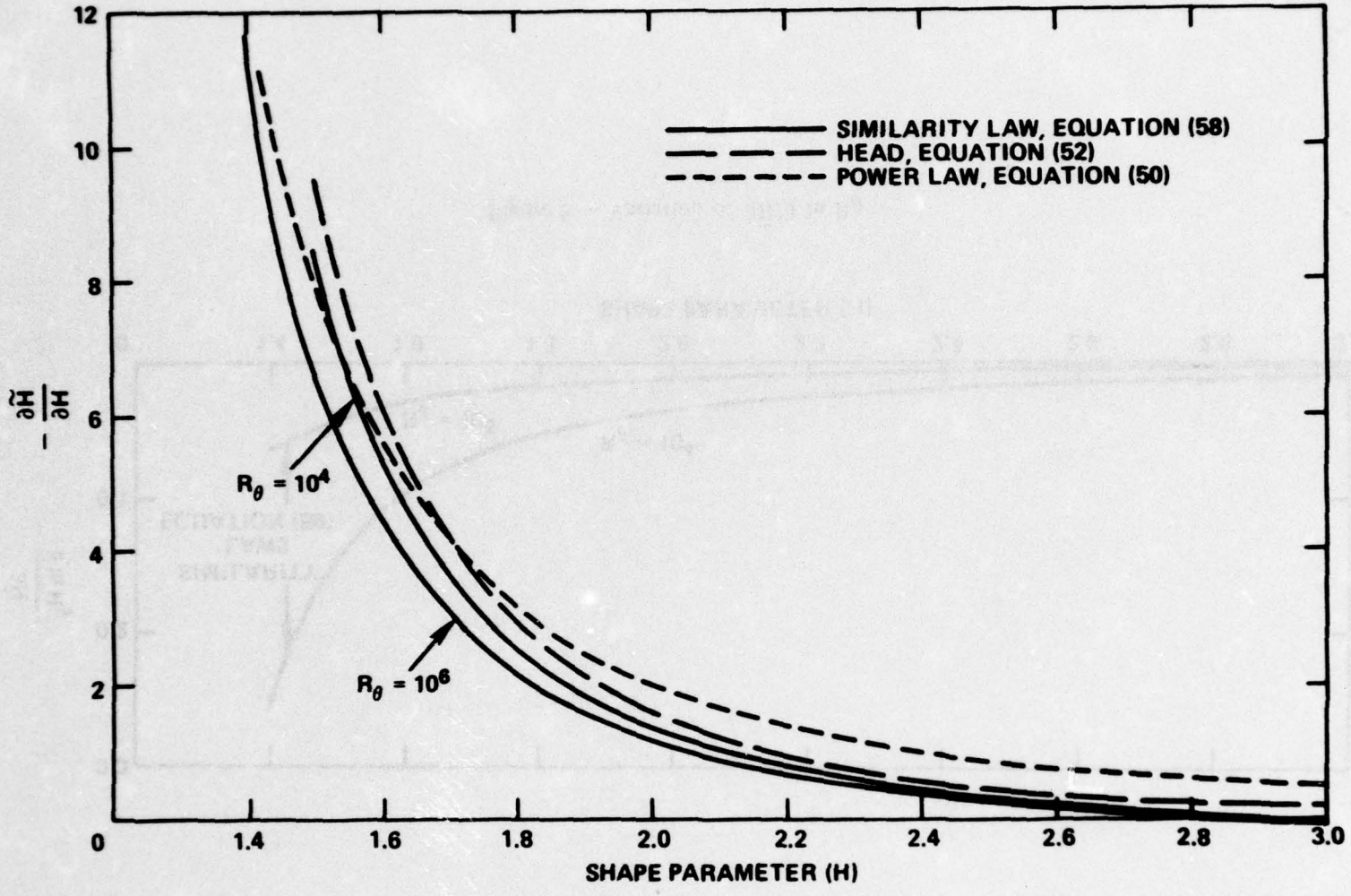

Figure 7 – Variation of $\partial\tilde{H}/\partial H$

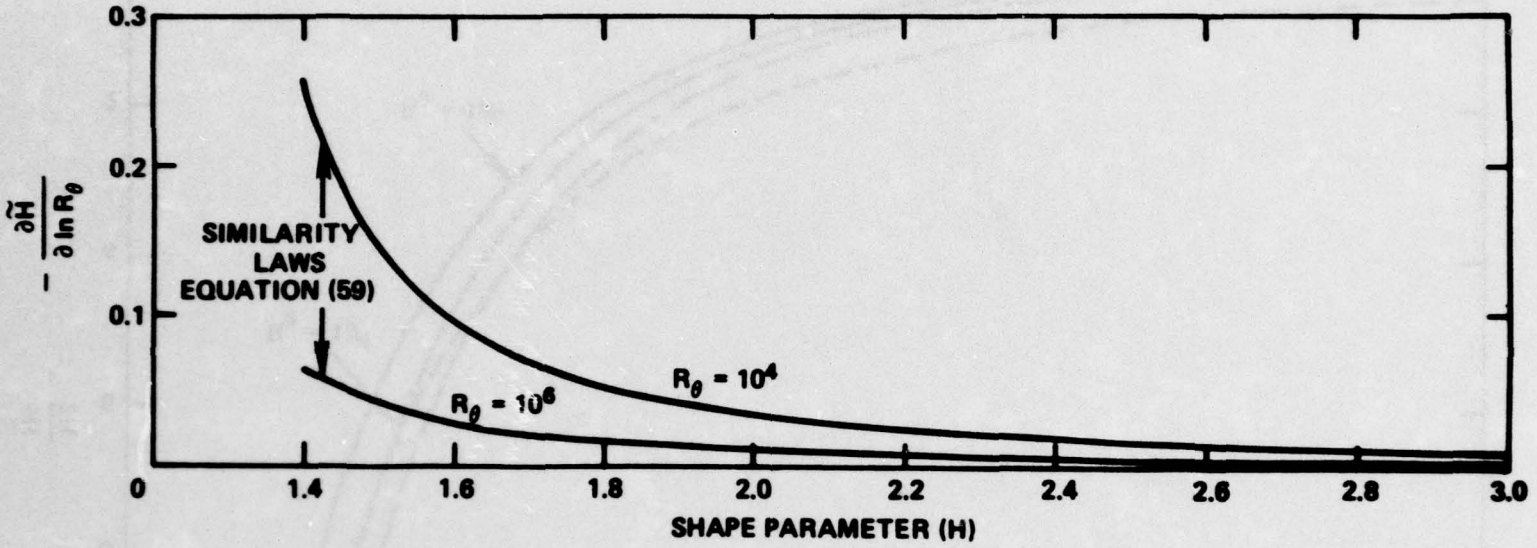

Figure 8 – Variation of $\partial \widetilde{H}/\partial \ln R_\theta$

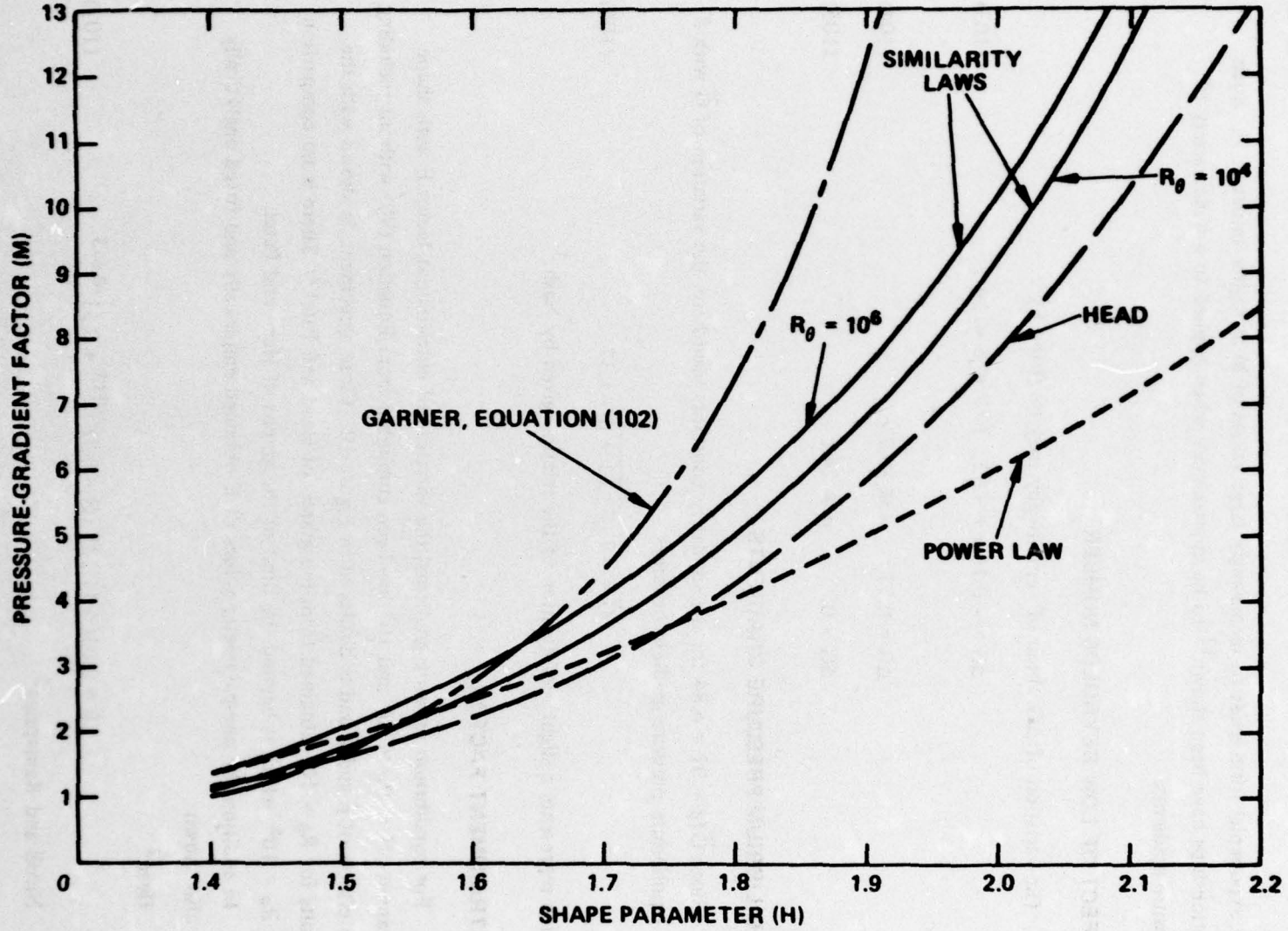

Figure 9 – Variation of Pressure-Gradient Factor

$$M = e^{5(H - 1.4)} \tag{102}$$

The exponenial form leads to increasingly large values of M at higher values of H. Such relationships have been shown[12] to be approximate when applied to a wide variety of pressure gradients.

EFFECT OF LOW REYNOLDS NUMBER

The variation of ΔG obtained[9] empirically may be fitted by

$$\Delta G = -0.16\sigma + 3.92, \quad 19.7 \leq \sigma \leq 24.5 \tag{103}$$

Also

$$\Delta G = 0.77, \quad \sigma \leq 19.7 \tag{104}$$

$$\Delta G = 0, \quad \sigma \geq 24.5 \tag{105}$$

EQUILIBRIUM PRESSURE GRADIENTS

Since $\tilde{G}[\beta = 0] = 6.84$ for the similarity constants used here, the variation of $\tilde{G}$ with β *for equilibrium pressure gradient* becomes

$$\tilde{G} = 6.1\sqrt{1.81 + \beta} - 1.37 \tag{106}$$

which represents a slight modification of the relation given by Nash.[3]

ENTRAINMENT FACTOR

For equilibrium pressure gradients, the variation of entrainment factor E with shape parameter H at $R_\theta = 10^4$ and 10^6 has been computed from Equation (90) without including the effects of $\hat{p}$ and $\hat{q}$ and is displayed in Figure 10. Close agreement, is shown with the results for $R_\theta = 10^4$ obtained from the graphs of Head and Patel.[2] There is no comparison for $R_\theta = 10^6$, which is beyond the limit of the graphs of Head and Patel.

In addition the one-parameter values of E obtained empirically and fitted analytically are also shown

Head[3]

$$E = 0.0306\,[1.535\,(H - 0.7)^{-2.715} + 0.3]^{-0.653} \tag{107}$$

Nicoll and Ramaprian[3]

$$E = 0.035\sqrt{H - 1.25} \tag{108}$$

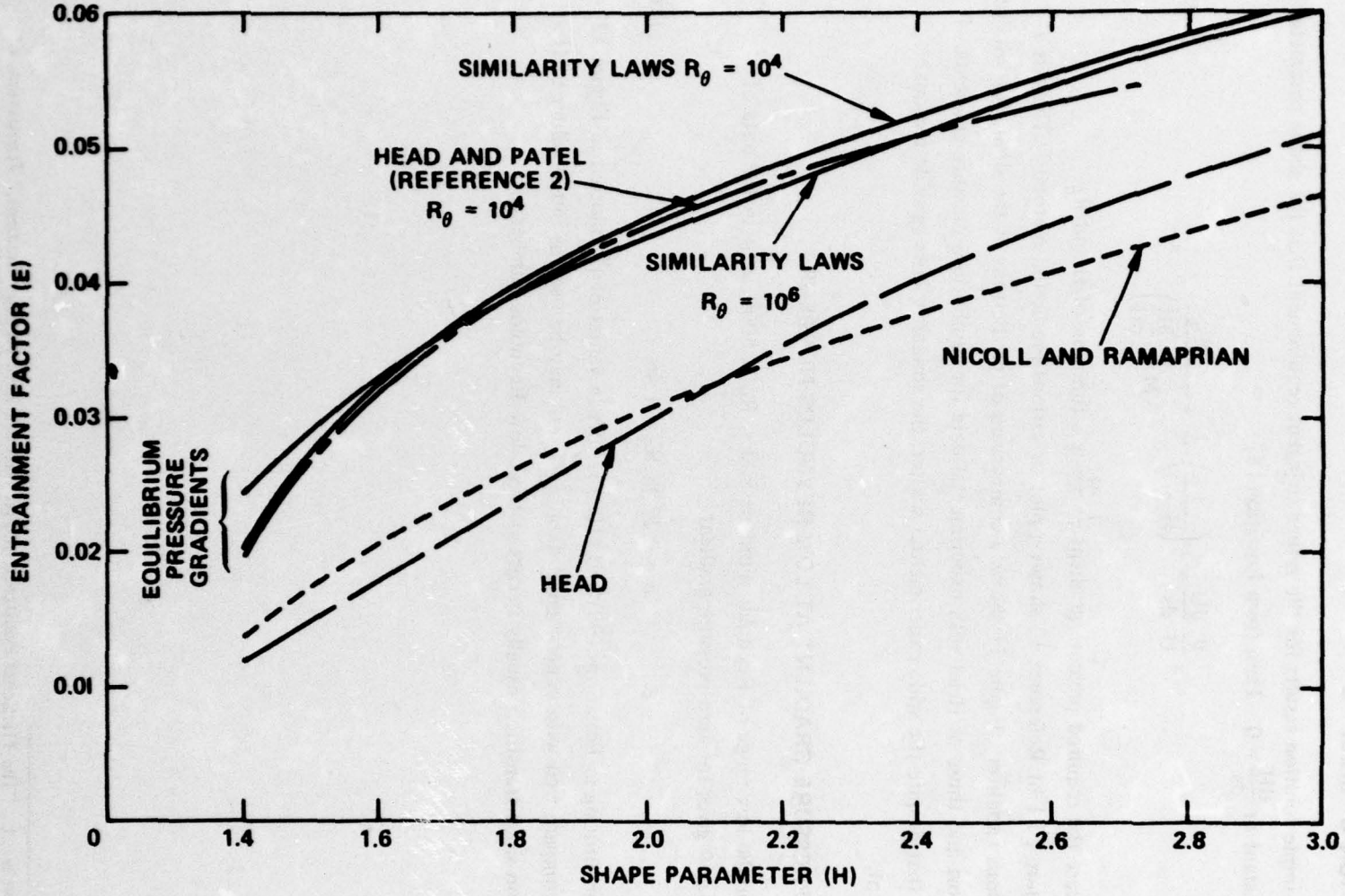

Figure 10 – Entrainment Factor

CONDITION OF dH/ds = 0

A simple solution results for the rather stringent requirement that the shape parameter H stay constant or $\frac{dH}{ds} = 0$. Then from Equation (87)

$$-\frac{\theta}{U}\frac{dU}{ds} = -\left(\frac{1}{H+1}\right)\frac{1}{\sigma^2} + \frac{E}{M\left(-\frac{\partial \tilde{H}}{\partial H}\right)} \tag{109}$$

In this case the required pressure gradient $\frac{\theta}{U}\frac{dU}{ds}$ is a function of H and R_θ.

Figure 22.1 of Reference 12 shows a plot of various prediction methods. There is a tremendous variation. Figure 11 shows a comparison of predictions of the similarity laws of this report and those of Head with experimental data for equilibrium pressure gradients. It is evident that despite the wide experimental scatter, the similarity laws provide reasonable agreement.

ZERO PRESSURE GRADIENT AT LOW REYNOLDS NUMBERS

For the low range of Reynolds numbers $800 < R_\theta < 5000$, a fit to the data of Reference 9 gives for zero pressure gradient

$$\sigma = 3.22 \ln R_\theta - 1.46 \tag{110}$$

Substituting in Equations (99) and (100) results in values of H_o plotted in Figure 12, which compare well with experimental data.[13] These may be used as initial values of H at transition since transition usually occurs at those low Reynolds numbers.

[13] Landweber, L., "The Frictional Resistance of Flat Plates in Zero Pressure Gradient," Transactions of Society of Naval Architects and Marine Engineers," Vol. 61, pp. 5-32 (1953).

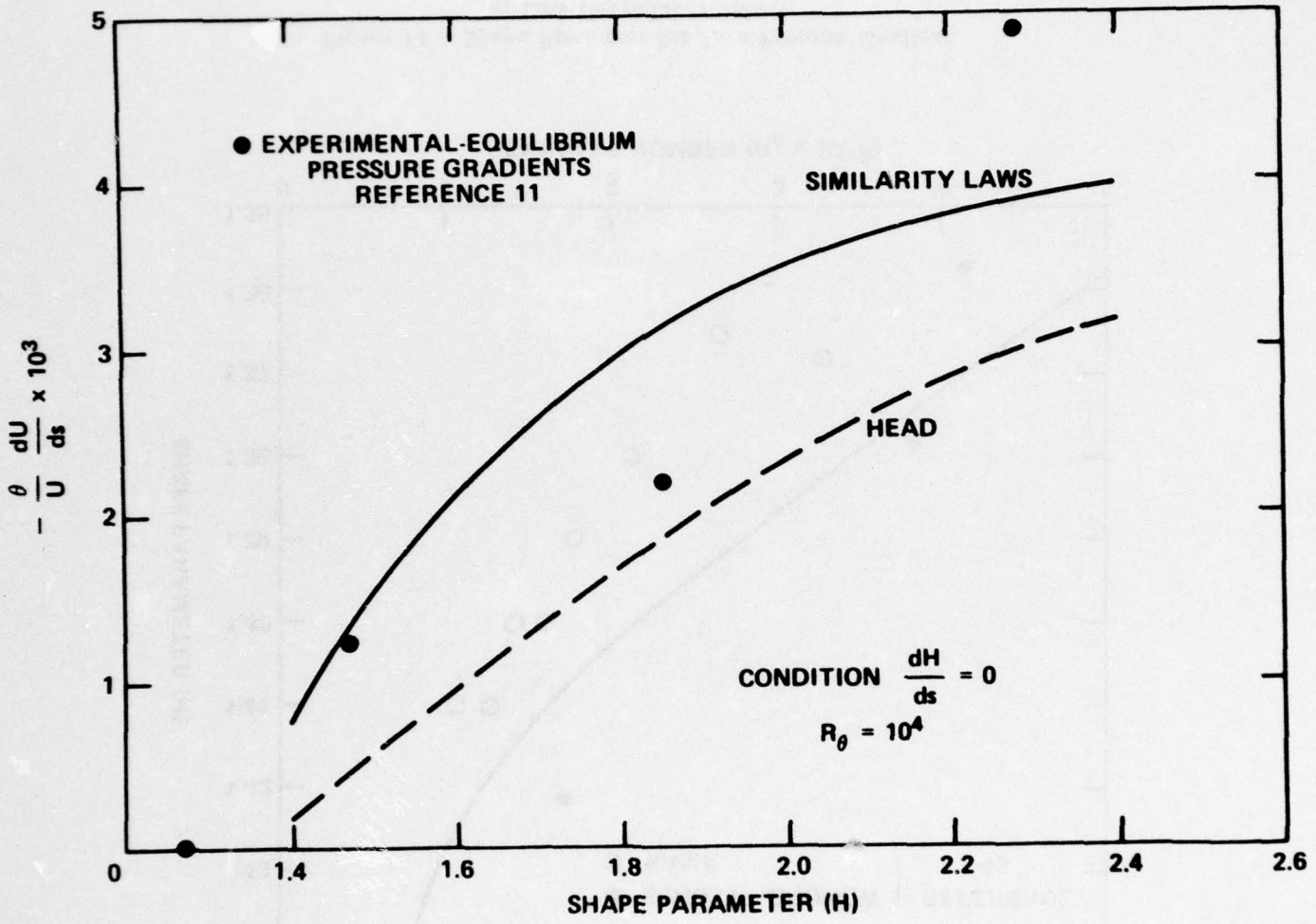

Figure 11 – Condition of dH/ds = 0

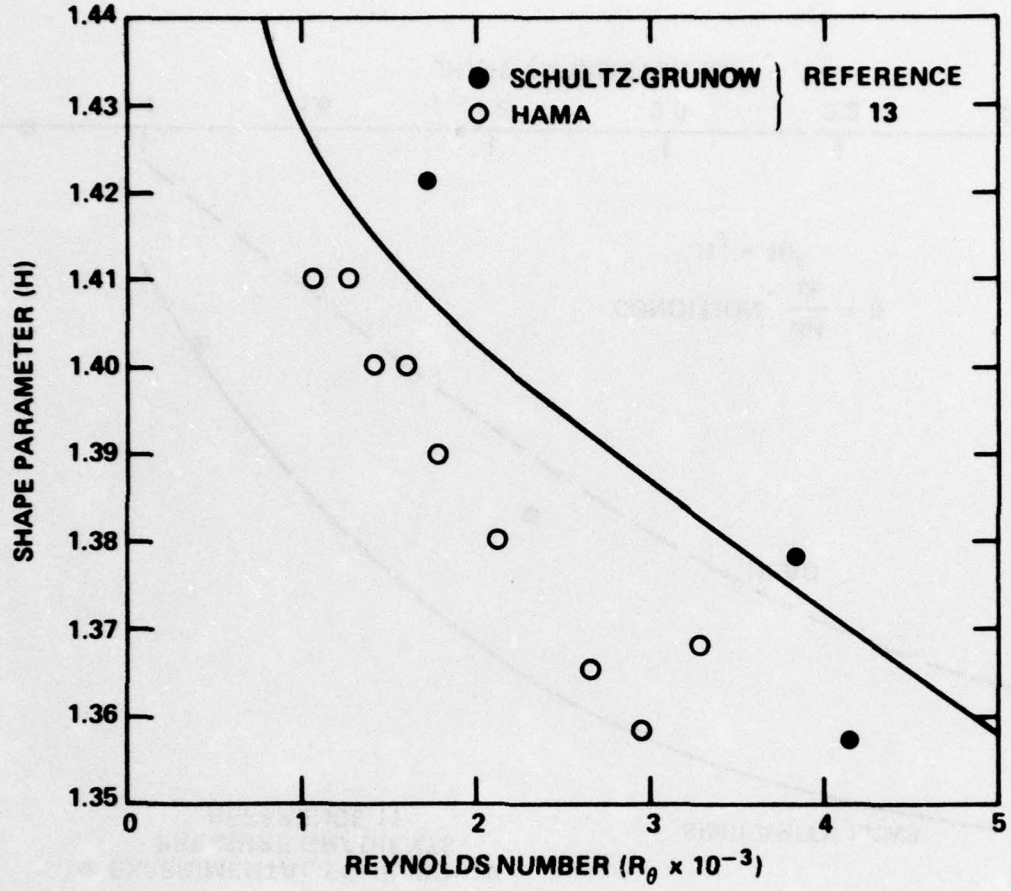

Figure 12 – Shape Parameter for Zero Pressure Gradient at Low Reynolds Numbers

SUMMARY

All the necessary analytical relations have been derived for the calculation of a two-dimensional turbulent boundary layer in a pressure gradient. From these relations, the variation of the momentum loss, the boundary layer thickness, the local skin friction, and the velocity profile may be calculated as a function of downstream position. The method is firmly founded on only fundamentals, the equations of motion for the boundary layer, the velocity similarity laws, and the characteristics of equilibrium pressure gradients which are well substantiated by experimental data. The two-parameter characterization should be sufficient for most engineering analyses of the two-dimensional turbulent boundary layer in pressure gradients. For the boundary layer close to separation, adequate formulations for the transverse pressure distribution and the normal turbulent stresses are still missing. Basing the equilibrium entrainment factor on H and R_θ only without a direct coupling to the pressure gradient should prove adequate for most pressure gradients found in engineering applications. For unusually large pressure gradients, however, adjustments may be needed to the equilibrium entrainment factor.

For convenience, the necessary analytical relations are listed in the appendix for the solution of the two simultaneous differential equations: the momentum and the shape parameter. Also included are the relations specifying the boundary-layer velocity profile at each streamwise position.

APPENDIX A
CALCULATION PROCEDURE

All the necessary analytical relations for calculating the development fo the two-dimensional turbulent boundary and the associated velocity profiles are now listed.

Solve as simultaneous equations for $\theta[s]$ and $H[s]$, given $U[s]$ and $\frac{dU}{ds}[s]$ ($\hat{p}$ and $\hat{\sigma}$ are assumed equal to zero).

$$\frac{d\theta}{ds} = -(H+2)\frac{\theta}{U}\frac{dU}{ds} + \frac{1}{\sigma^2} \tag{4}$$

$$\theta\frac{dH}{ds} = -M\frac{\theta}{U}\frac{dU}{ds} + \left(\frac{M}{H+1}\right)\frac{1}{\sigma^2} - E_e\left(-\frac{\partial\tilde{H}}{\partial H}\right)^{-1} \tag{87}$$

where

$$M = (H+1)\left(\tilde{H} + \frac{\partial\tilde{H}}{\partial \ln R_\theta}\right)\left(-\frac{\partial\tilde{H}}{\partial H}\right)^{-1} \tag{88}$$

$$E_e = \left\{\tilde{H} + \frac{\partial\tilde{H}}{\partial \ln R_\theta} - \left(\frac{\partial\tilde{H}}{\partial H}\right)\left[\frac{A\,H(H-1)^2}{A(H-1)^2 + G\,H}\right]\right\}\left\{\left[1 + \frac{(H+1)}{H}\beta\right]\frac{1}{\sigma^2}\right\} \tag{90}$$

$$\beta = \left(\frac{\tilde{G} + a_3}{a_1}\right)^2 - a_2 \tag{95}$$

$$\tilde{G} = G + \Delta G \tag{94}$$

$$\Delta G = 0.16\sigma + 3.92, \quad 19.7 \leq \sigma \leq 24.5 \tag{102}$$

$$\Delta G = 0.77, \quad \sigma \leq 19.7 \tag{103}$$

$$\Delta G = 0, \quad \sigma \geq 24.5 \tag{104}$$

$$G = \sigma\left(1 - \frac{1}{H}\right) \tag{39}$$

$$\tilde{H} = \left(\frac{H^2}{H-1}\right)\left(1.4857 + \frac{0.4739\,A}{G} + \frac{5A^2}{G^{2.75}}\right) - H \tag{57}$$

$$\frac{\partial\tilde{H}}{\partial H} = \frac{\tilde{H}(H-2) - H}{H(H-1)} - \left(\frac{H^2}{H-1}\right)\left(\frac{0.4739\,A}{G} + \frac{13.75\,A^2}{G^{2.75}}\right)\left(\frac{1}{H(H-1)} + \frac{\partial \ln \sigma}{\partial H}\right) \tag{58}$$

$$\frac{\partial \tilde{H}}{\partial \ln R_\theta} = -\left(\frac{H^2}{H-1}\right)\left(\frac{0.4739\,A}{G} + \frac{13.75\,A^2}{G^{2.75}}\right)\frac{\partial \ln \sigma}{\partial \ln R_\theta} \tag{59}$$

$$\frac{0.3462(3.889-H)}{H}\sigma + 0.9392\,A \ln \sigma = A \ln R_\theta + B_1 - 2.0938\,A - A \ln\left[\frac{(H-1)^{0.9392}}{H^{1.9392}}\right] \tag{66}$$

$$\frac{\partial \ln \sigma}{\partial H} = \frac{2.8885}{H(H-1)}\left[\frac{1.3462(H-1)\sigma + A\,H(H-1.9392)}{(3.889-H)\sigma + 2.7129\,A\,H}\right] \tag{74}$$

$$\frac{\partial \ln \sigma}{\partial \ln R_\theta} = \frac{2.8885\,A\,H}{(3.889-H)\sigma + 2.7129\,A\,H} \tag{75}$$

$A = 2.606,\ B_1 = 3.88$

$a_1 = 6.1,\ a_2 = 1.81,\ a_3 = 1.37$

INITIAL CONDITIONS AT TRANSITION

$$\left(\frac{U\theta}{\nu}\right)_{turb} = (R_\theta)_{turb} = (R_\theta)_{lam} + \Delta R_\theta \tag{97}$$

$$\frac{1}{H_o} = 1 - \frac{\tilde{G}_o - \Delta G[\sigma_o]}{\sigma_o} \tag{99}$$

$$\tilde{G}_o = 6.84$$

$$\Delta G = -0.16\,\sigma_o + 3.92 \tag{102}$$

$$\sigma_o = 3.22 \ln R_\theta - 1.46 \tag{109}$$

VELOCITY PROFILE

At each station s, H, θ, σ and G have been calculated. Then from Equation (56)

$$I_1 = \frac{G}{1.4857 + \frac{0.4739\,A}{G} + \frac{5A^2}{G^{2.75}}}$$

from Equation (44)

$$B_2 = 2I_1 - \frac{11}{6}A$$

From definitions

$$u_\tau = \frac{U}{\sigma}$$

From Equation (60)

$$\eta = \frac{u_\tau \delta}{\nu} = e^{\frac{\sigma - B_1 - B_2}{A}}$$

Then

$$\delta = \frac{\eta \nu}{u_\tau}$$

For $y^* > y_o^*$

$$y^* = \frac{u_\tau y}{\nu}$$

$$\frac{u}{u_\tau} = A \ln y^* + B_1 + B_2 \frac{w}{2} + Aq, \qquad y_o^* \leq y^* \leq \eta \tag{30a}$$

$$\frac{w}{2} = 3\left(\frac{y}{\delta}\right)^2 - 2\left(\frac{y}{\delta}\right)^3 \tag{31}$$

$$q = \left(\frac{y}{\delta}\right)^2 \left(1 - \frac{y}{\delta}\right) \tag{32}$$

For $y^* \leq y_o^*$ (Reference 6)

laminar sublayer, $\quad \frac{u}{u_\tau} = y^* \qquad o \leq y^* \leq y_L^*$

buffer sublayer $\quad \frac{u}{u_\tau} = A \ln (y^* - J) + B_1, \quad y_L^* \leq y^* \leq y_o^*$

$$J = B_1 + A \ln A - A$$

$$y_L^* = B_1 + A \ln A$$

More simply let

$$\frac{u}{u_\tau} = A \ln (y^* - J) + B_1 + B_2 \frac{w}{2} + Aq, \quad y_L^* \leq y^* \leq \eta$$

for the boundary layer outside the laminar sublayer.

REFERENCES

1. Head, M.R., "Entrainment in the Turbulent Boundary Layer," Aeronautical Research Council R&M 3152 (Sep 1958).

2. Head, M.R. and V.C. Patel, "Improved Entrainment Method for Calculating Turbulent Boundary Layer Development," Aeronautical Research Council R&M 3643 (Mar 1968).

3. Granville, P.S., "Integral Methods for Turbulent Boundary Layers in Pressure Gradients," Journal of Ship Research, Vol. 16, No. 3, pp. 191-204 (Sep 1972).

4. Granville, P.S., "A Modified Law of the Wake for Turbulent Shear Flow," NSRDC Report 4639 (Sep 1975).

5. Schlichting, H., "Boundary-Layer Theory," Sixth Edition, McGraw-Hill Book Co., New York (1968).

6. Granville, P.S., "The Frictional Resistance and Turbulent Boundary Layer of Rough Surfaces," Journal of Ship Research, Vol. 2, No. 3, pp. 52-74 (Dec 1958).

7. Granville, P.S., "The Frictional Resistance and Velocity Similarity Laws of Drag-Reducing Polymer Solutions," Journal of Ship Research, Vol. 12, No. 3, pp. 201-212 (Sep 1968).

8. "Proceedings–Computation of Turbulent Boundary Layers, 1968 AFOSR-IFP Stanford Conference," Edited by Kline, S.J. et al., Vol. 1, Thermosciences Division, Stanford University (1968).

9. Granville, P.S., "The Drag and Turbulent Boundary Layer of Flat Plates at Low Reynolds Numbers," DTNSRDC Report 4682 (Dec 1975).

10. Cebeci, T. and G.J. Mosinskis, "Computation of Incompressible Turbulent Boundary Layers at Low Reynolds Numbers," American Institute of Aeronautics and Astronautics Journal, Vol. 9, No. 8, pp. 1632-1634 (Aug 1971).

11. "Proceedings–Computation of Turbulent Boundary Layers, 1968 AFOSR-IFP Stanford Conference," Edited by Coles, D.E. and E.A. Hirst, Vol. 2, Thermosciences Division, Stanford University, (1968).

12. Rotta, J.C., "Turbulent Boundary Layers in Incompressible Flow," Chapter in Progress in Aeronautical Sciences, Vol. 2, Edited by A. Ferri, et al., Pergamon Press, New York (1962).

13. Landweber, L., "The Frictional Resistance of Flat Plates in Zero Pressure Gradient," Transactions of Society of Naval Architects and Marine Engineers," Vol. 61, pp. 5-32 (1953).

INITIAL DISTRIBUTION

Copies	
1	U.S. ARMY TRANS R&D Marine Trans Div
1	DOD, ARPA
4	CHONR 3 Code 438 1 Code 460
1	NRL
1	USNA 1 Bruce Johnson
1	NAVPGSCOL
1	NROTC & NAVADMINU, MIT
1	NAVWARCOL
1	NELC
5	NAVUSEACEN San Diego 1 A.G. Fabula 1 *T. Lang* 1 J.W. Hoyt 1 G.L. Donahue
1	NAVWPNSCEN
2	NSWC White Oak 1 V.C. Dawson 1 J.E. Goeller
3	NUSC NPT 1 P. Gibson 1 J.F. Brady 1 R.H. Nadolink
1	NLONLAB NUSC
9	NAVSEASYSCOM 2 SEA 09G32 1 SEA 03C 1 SEA 03 2 SEA 033 1 SEA 035A 2 PMS-395
2	NAVAIRSYSCOM

Copies	
4	NAVSEC 1 SEC 6110.01 1 SEC 6114 1 SEC 6114D 1 SEC 6115
2	AFSOR 1 Code 518
12	DDC
3	Bureau of Standards 1 Mechanics Div 1 P.S. Klebanoff 1 G. Kulin
1	MARAD Div of Ships R&D
2	NASA HQS 1 A. Gessow
1	National Science Foundation *Eng Sci Div*
1	Univ of Bridgeport E.M. Uram, Dept Mech Eng
2	Univ of Calif Berkeley Dept of NA
3	Calif Inst of Technol 1 A.J. Acosta 1 Sabersky 1 D. Coles
3	Catholic Univ Dept of Mech Eng 1 M.J. Casarella 1 P.K. Chang
2	Davidson Lab, Stevens Inst of Tech
2	Iowa State Univ Inst of Hydraulic Res 1 L. Landweber 1 V.C. Patel

Copies	
4	Mass Inst of Technol Dept of Ocean Eng 1 Lib 1 J.N. Newman 1 P. Mandel 1 M. Abkowitz
2	Univ of Michigan Dept of NAME
1	Univ of Minnesota St. Anthony Falls Hydr Lab 1 R. Arndt
3	Penn State Univ Applied Research Lab 1 J.L. Lumley 1 R.E. Henderson 1 B.R. Parkin
2	Univ of Rhode Island 1 F.M. White, Dept Mech Eng 1 T. Kowalski, Dept Ocean Eng
2	Stanford Univ 1 E.Y. Hsu, Dept Civil Eng 1 S.J. Kline, Dept Mech Eng
2	VPI 1 H.L. Moses, Dept Mech Eng 1 D.P. Telionis, Dept Eng Sci
2	Worcester Polytech Inst Alden Res Labs 1 L.C. Neale
1	SNAME
1	Douglas Aircraft, Long Beach, Calif.
1	Exxon Math & Systems, Inc R. Bernicker
2	Hydronautics, Inc 1 M.P. Tulin 1 R. Barr
1	Adv Tech Center C.S. Wells, Jr.
1	Oceanics, Inc A. Lehman

Copies	
3	Rand Corp 1 E.R. van Driest 1 C. Gazley 1 J. Aroesty
1	Westinghouse Electric 1 M.S. Macovsky

CENTER DISTRIBUTION

Copies	Code	
1	012	
1	1500	
1	1504	
1	1520	
1	1540	
100	1541	P.S. Granville
3	1552	J.H. McCarthy
1	1556	
1	1560	
1	1802.2	
1	1802.3	
1	1802.4	
1	1843	
1	1900	
1	1940	
1	1942	
30	5214.1	Reports Distribution
1	5221	Library (C)
1	5222	Library (A)